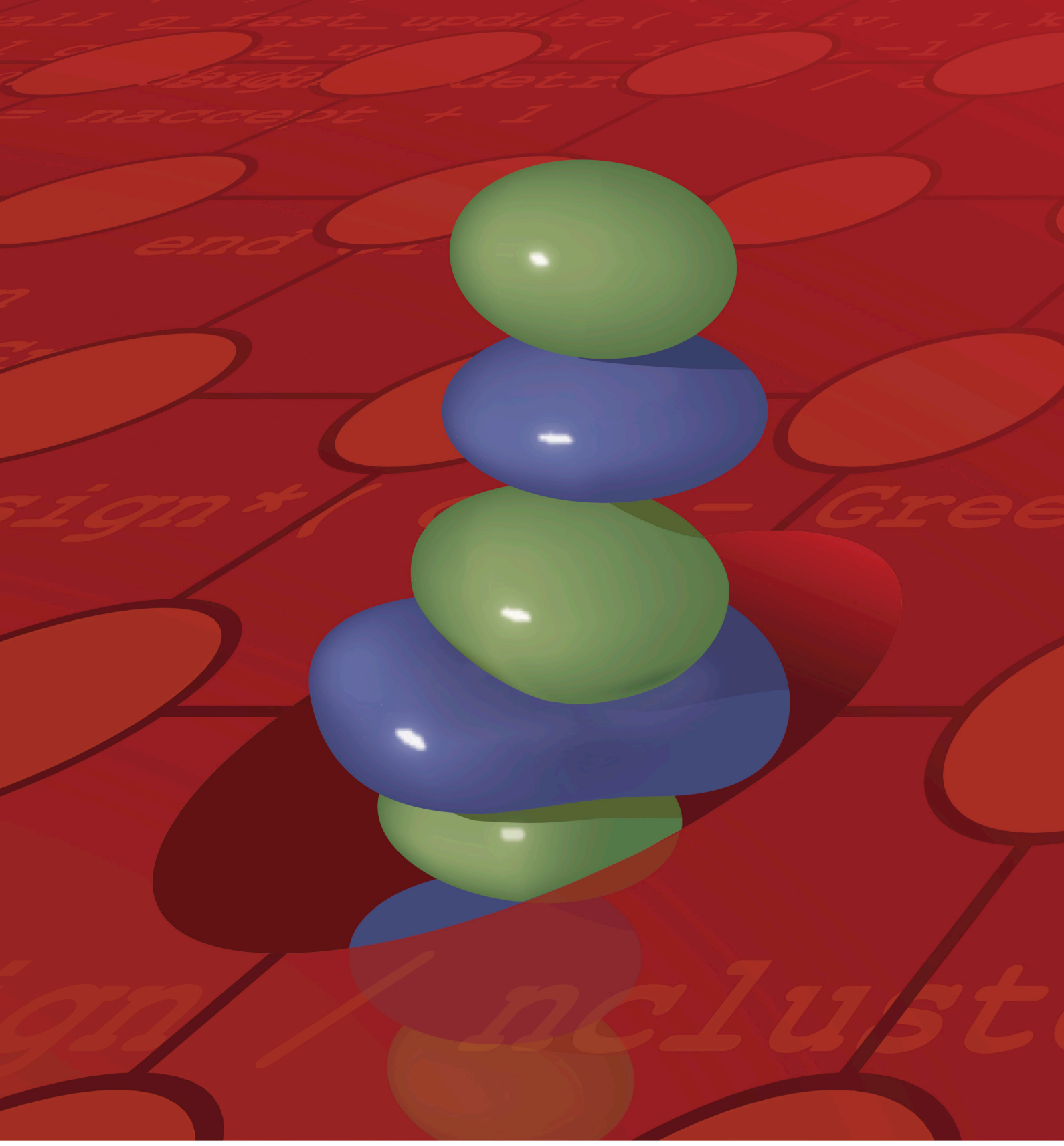

Understanding Correlated Materials with DMFT

Eva Pavarini, Erik Koch, Alexander Lichtenstein, and Dieter Vollhardt (Eds.)

JÜLICH
Forschungszentrum

Schriften des Forschungszentrums Jülich
Reihe Modeling and Simulation Band / Volume 15

Forschungszentrum Jülich GmbH
Peter Grünberg Institute
Jülich Supercomputing Centre

Lecture Notes of the Autumn School on Correlated Electrons 2025

Eva Pavarini, Erik Koch, Alexander Lichtenstein, and Dieter Vollhardt (Eds.)

Understanding Correlated Materials with DMFT

Autumn School organized by
the Peter Grünberg Institute
at Forschungszentrum Jülich
22 – 26 September 2025

Schriften des Forschungszentrums Jülich
Modeling and Simulation Band / Volume 15

ISSN 2192-8525 ISBN 978-3-95806-813-1

Bibliographic information published by the Deutsche Nationalbibliothek.
Die Deutsche Nationalbibliothek lists this publication in the Deutsche Nationalbibliografie; detailed bibliographic data are available in the Internet at http://dnb.d-nb.de.

Publisher:	Forschungszentrum Jülich GmbH Jülich Supercomputing Centre
Cover Design:	Grafische Medien, Forschungszentrum Jülich GmbH
Printer:	Schloemer & Partner GmbH, Düren
Copyright:	Forschungszentrum Jülich 2025
Distributor:	Forschungszentrum Jülich Zentralbibliothek, Verlag 52425 Jülich Phone +49 (0)2461 61-5368 · Fax +49 (0)2461 61-6103 e-mail: zb-publikation@fz-juelich.de www.fz-juelich.de/zb

Schriften des Forschungszentrums Jülich
Reihe Modeling and Simulation, Band / Volume 15

ISSN 2192-8525
ISBN 978-3-95806-813-1

Vollständig frei verfügbar über das Publikationsportal des Forschungszentrums Jülich (JuSER) unter www.fz-juelich.de/zb/openaccess

Contents

Preface

Dynamical mean-field theory (DMFT) has established itself as the method of choice for understanding emergent phases in correlated materials. In fact, its combination with density-functional theory (DFT) via the construction of materials-specific many-body Hamiltonians has opened the path to the description of correlation effects beyond the level of generic models. This, together with the development of powerful quantum-impurity solvers, and the help of modern massively-parallel supercomputers, provides powerful tools for unraveling correlation effects and has revolutionized the field of correlated materials science. The goal of this year's school is to provide students with an overview of the method and its application to materials, with a view towards the future of many-body simulations. The program will start with fundamental models and concepts, introducing the Hubbard model, density-functional theory and the principles of DMFT. More advanced lectures will focus on the DFT+DMFT technique and its extensions. Specialized lectures will then demonstrate how the approach can be used to identify the mechanism of paradigmatic emergent phenomena in materials: non-conventional superconductivity, orbital ordering, Mott phases, disorder, Hund's metal behavior, and pseudogap phases. The topics will be treated with a focus on explaining key experiments in a realistic setting and with an outlook on materials design.

A school of this size and scope requires backing from many sources. We are very grateful for all the practical and financial support we have received. The Peter Grünberg Institute at the Forschungszentrum Jülich and the Jülich Supercomputing Centre provided the major part of the funding and were vital for the organization of the school as well as for the production of this book. The Institute for Complex Adaptive Matter (ICAM) continued also this year to support the school and supplied additional funds.

The nature of a school makes it desirable to have the lecture notes available when the lectures are given. This way students get the chance to work through the lectures thoroughly while their memory is still fresh. We are therefore extremely grateful to the lecturers that, despite tight deadlines, provided their manuscripts in time for the production of this book. We are confident that the lecture notes collected here will not only serve the participants of the school but will also be useful for other students entering the exciting field of strongly-correlated materials.

We are grateful to Mrs. J. Timmer of the Verlag des Forschungszentrum Jülich and to Mrs. D. Mans of the Grafische Betriebe for providing their expert support in producing the present volume on a tight schedule. We heartily thank our students and postdocs who helped with proofreading the manuscripts, often on quite short notice: Elaheh Adibi, Amit Chauhan, Qiwei Li, and Xue-Jing Zhang.

Finally, our special thanks go to Dipl.-Ing. R. Hölzle for his invaluable advice on the innumerable questions concerning the organization of such an endeavor, and to Mrs. L. Snyders for expertly handling all practical issues.

Eva Pavarini, Erik Koch, Alexander Lichtenstein, and Dieter Vollhardt

August 2025

1 Understanding Correlated Materials with Lattice Fermions in Infinite Dimensions

Dieter Vollhardt
Center for Electronic Correlations and Magnetism
University of Augsburg

Contents

E. Pavarini, E. Koch, A. Lichtenstein, and D. Vollhardt (eds.)
Understanding Correlated Materials with DMFT
Modeling and Simulation Vol. 15
Forschungszentrum Jülich, 2025, ISBN 978-3-95806-813-1
http://www.cond-mat.de/events/correl25

1 Electronic correlations

1.1 Correlated materials

The effective interaction between electrons in solids differs significantly from the bare classical Coulomb interaction, since it depends not only on material-specific properties such as the electronic band structure and screening but, more generally, on exchange and correlation effects. Materials whose properties are strongly influenced by electronic correlations are referred to as "correlated electron materials", or simply "correlated materials".

It has long been known that correlation effects are strong in materials with partially filled d and f electron shells and narrow energy bands as in the $3d$ transition metals [1] or the rare–earths [2] and their compounds. But more recently it was found that strong electronic correlations can occur even in materials without transition metal or rare-earth elements, such as "Moiré" (or, more generally, twisted) van der Waals heterostructures [3].

Electronic correlations in solids often result in complex physics such as heavy fermion behavior and unconventional superconductivity [4], especially high temperature superconductivity [5], colossal magnetoresistance [6], Mott metal-insulator transitions [7], the fractional quantum Hall effect [8], and Fermi liquid instabilities [9]. The recent discovery of correlation phenomena and rich phase diagrams in Moiré heterostructures [3] has further increased the interest in correlation physics.

The exceptional properties of correlated materials are not only of interest for fundamental research but may also be relevant for technological applications. Namely, the unusual sensitivity of correlated electron materials upon changes of external parameters such as temperature, pressure, electromagnetic fields, and doping can be employed to develop materials with useful functionalities [10]. For example, Moiré heterostructures may enable "twistronics", a new approach to device engineering [11]. Consequently there is a great need for the development of appropriate models and theoretical investigation techniques which allow for a comprehensive and at the same time reliable exploration of correlated materials [12].

1.2 The many-electron problem

The investigation of electronic correlation effects in solids requires the application of quantum many-body theory for electrons ("many-electron theory"). This is faced by two closely connected problems: the need for a sufficiently simple model of correlated electrons and its solution. Progress in this direction was remarkably slow.[1] A microscopic model of corre-

[1] Given the fact that the Heisenberg model [13], which explains ferromagnetic order of localized spins in solids as the result of quantum-mechanical exchange processes, had been introduced already in 1928, and Bloch's [14] subsequent observation that a model for ferromagnetism in $3d$ transition metals had to include the mobile nature of the electrons, one might naively expect that this set the stage for the rapid formulation of a correlated electron model and its approximate investigation. But this was not the case (for a historical review of the evolution of the quantum-mechanical theory of metals from 1928 to 1933, which describes the conceptual problems of that time, see ref. [15]). One reason for the slow development of a many-electron theory was that in the 1930s and 40s nuclear physics attracted more attention than solid-state physics, with a very specific focus of research during the 2nd World War. But apart from that, the sheer complexity of the many-body problem itself did not allow for

lated electrons did not emerge until 1963, when a lattice model was proposed independently by Gutzwiller [17], Hubbard [18], and Kanamori [19] to explain ferromagnetism in $3d$ transition metals. Today this model is referred to as "Hubbard model".

2 The minimal model for interacting lattice electrons

Fermionic particles that move and interact on a lattice rather than in the continuum are referred to as "lattice fermions". The minimal microscopic model of interacting lattice fermions is the single-band Hubbard model. The Hamiltonian consists of the kinetic energy $\hat{H}_0$ and the interaction energy $\hat{H}_{\rm int}$ (in the following operators are denoted by a hat)

$$\hat{H} = \hat{H}_0 + \hat{H}_{\rm int}, \tag{1a}$$

$$\hat{H}_0 = \sum_{\boldsymbol{R}_i,\boldsymbol{R}_j,\sigma} t_{ij}\, \hat{c}^\dagger_{i\sigma}\hat{c}_{j\sigma} = \sum_{\boldsymbol{k},\sigma} \varepsilon_{\boldsymbol{k}}\hat{n}_{\boldsymbol{k}\sigma}, \tag{1b}$$

$$\hat{H}_{\rm int} = U\sum_{\boldsymbol{R}_i} \hat{n}_{i\uparrow}\hat{n}_{i\downarrow} \equiv U\hat{D}. \tag{1c}$$

Here $\hat{c}^\dagger_{i\sigma}(\hat{c}_{i\sigma})$ are creation (annihilation) operators of fermions with spin σ at site $\boldsymbol{R}_i$ (for simplicity denoted by i), $\hat{n}_{i\sigma} = \hat{c}^\dagger_{i\sigma}\hat{c}_{i\sigma}$, and $\hat{D} = \sum_{\boldsymbol{R}_i}\hat{D}_i$ is the operator of total double occupation of the system with $\hat{D}_i = \hat{n}_{i\uparrow}\hat{n}_{i\downarrow}$ as the operator of double occupation of a lattice site i. The Fourier transform of the kinetic energy in (1b), where t_{ij} is the amplitude for hopping between sites i and j, defines the dispersion $\varepsilon_{\boldsymbol{k}}$ and the momentum distribution operator $\hat{n}_{\boldsymbol{k}\sigma}$ with $\boldsymbol{k}$ as the wave vector. In the following the hopping is restricted to nearest-neighbor sites i and j, such that $-t \equiv t_{ij}$. A schematic picture of the Hubbard model is shown in Fig. 1.

2.1 Unique features of the Hubbard model

In the Hubbard model the Coulomb interaction between two electrons is assumed to be so strongly screened that it can be described by a local interaction U which occurs only *on* a lattice site.[2] Due to the Pauli exclusion principle such an on-site interaction is only possible if the two electrons have opposite spin. Thus it seems as if the interaction between the electrons was spin-dependent. But the Coulomb interaction is, of course, a spin-independent two-body interaction; the fact that the operators in (1c) contain spin indices is merely a consequence of the quantum mechanical treatment of electrons in a localized basis. A special feature of a purely

quick successes. High hurdles had to be overcome, both regarding the development of appropriate mathematical techniques (field-theoretic and diagrammatic methods, Green functions, etc.) and physical concepts (multiple scattering, screening of the long-range Coulomb interaction, quasiparticles and Fermi liquid theory, electron-phonon coupling, superconductivity, metal-insulator transitions, disorder, superexchange, localized magnetic states in metals, etc.). A discussion of the many-body problem and of some of the important developments up to 1961 can be found in the lecture notes and reprint volume by Pines [16].

[2] For that reason the Hubbard model applies particularly well to cold fermionic atoms in optical lattices where the bare interaction is indeed extremely short-ranged [20].

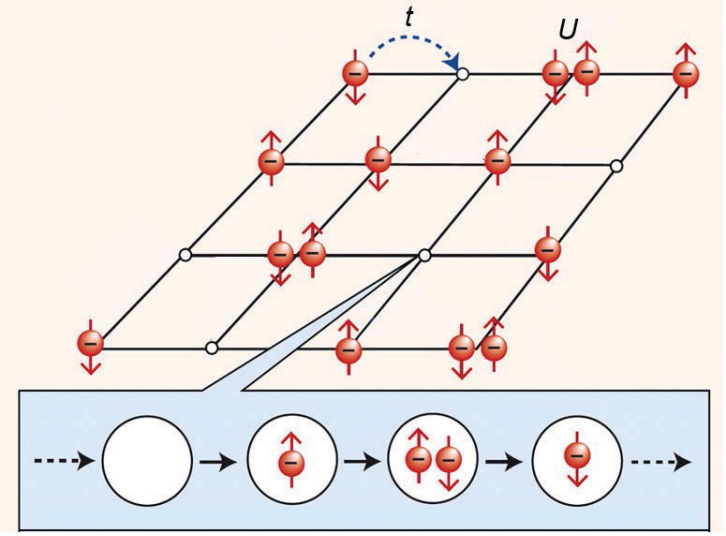

Fig. 1: *Schematic illustration of interacting electrons in a solid described by the Hubbard model. The ions enter only as a rigid lattice, here represented by a square lattice. The electrons, which have mass, negative charge, and spin (↑ or ↓), are quantum particles which tunnel ("hop") from one lattice site to the next with a hopping amplitude t. Together with the lattice structure this determines the band structure of the non-interacting electrons. The quantum dynamics leads to fluctuations in the occupation of lattice sites as indicated by the sequence at the bottom: a lattice site can either be unoccupied, singly occupied (↑ or ↓), or doubly occupied. When two electrons meet on a lattice site, which is only possible if they have opposite spins because of the Pauli exclusion principle, they encounter a local interaction U.*

local interaction is its complete independence of the lattice structure and spatial dimension of the system.

The physics described by the Hubbard model is clearly very different from that of electrons with a long-range Coulomb interaction in the continuum. Therefore the Hubbard model is far from obvious. Its formulation required fundamentally new insights into the nature of the many-body problem of interacting fermions (see footnote 1). In particular, screening is a basic ingredient of the many-body problem of metals.[3]

While the kinetic energy $\hat{H}_0$ is diagonal in momentum space and reflects the wave nature of the electrons, the interaction energy $\hat{H}_{\rm int}$ is diagonal in position space and characterizes their particle properties. In view of the uncertainty principle the two parts of the Hamiltonian are therefore maximally "quantum incompatible".

[3]It should be noted that Anderson had introduced the main ingredient of the Hubbard model, namely a local interaction between spin-up and spin-down d electrons with strength U, already in his 1959 paper on the theory of superexchange interactions [21] and, even more explicitly in his 1961 paper on localized magnetic states in metals, where he formulated a model of s and d electrons referred to today as "single impurity Anderson Model" (SIAM) or "Anderson impurity model" (AIM) [22]. The latter paper inspired Wolff [23] to study the formation of localized magnetic moments in dilute alloys in terms of a model with a single-band of noninteracting d electrons which can interact only on a single site. In this sense the Hubbard model could be called "periodic Wolff model" in analogy to the standard terminology "periodic Anderson model", which generalizes the AIM by extending the interaction to all sites of the lattice. Apparently Gutzwiller, Hubbard and Kanamori did not know the earlier work of Anderson and Wolff; at least they did not refer to their papers.

The Coulomb interaction between electrons with equal spin direction, e.g., on neighboring sites, is not described by the Hubbard model, but can be easily included. Similarly, the model can be generalized to more than one band. Indeed, in a Wannier basis the Hubbard model can be derived systematically from a general Hamiltonian of interacting electrons which consists of a kinetic energy, the ionic potential $U_{\text{ion}}(\boldsymbol{r})$, and the two-body Coulomb interaction $V_{\text{ee}}(\boldsymbol{r}-\boldsymbol{r}')$ [18]; for a discussion see ref. [24].

As mentioned above, the Hubbard model was originally introduced to provide a microscopic explanation of ferromagnetism in $3d$ transition metals [17–19]. Indeed, taken by itself the Hubbard interaction favors a ferromagnetic ground state, since this corresponds to the state with the lowest (zero) energy due to the absence of doubly occupied sites. However, this argument ignores the other term in the Hamiltonian, the kinetic energy. While the lattice structure and spatial dimension do not influence the Hubbard interaction, they play a very important role in the kinetic energy, where they determine, for example, the density of states of the electronic band at the Fermi energy (see section 5).

The single-band Hubbard model is the fundamental lattice model of interacting fermions.[4] As a consequence, many well-known models can be derived from it in special limits of the model parameters. For example, at half filling and in the limit $U \gg t$ the Hubbard model corresponds to the Heisenberg model with antiferromagnetic exchange coupling $J = 4t^2/U$.

2.1.1 How can the Hubbard model be solved?

In spite of the extreme simplifications of the Hubbard model compared with interacting electrons in a real solid, the model still cannot be solved analytically, except in dimension $d=1$ for nearest-neighbor hopping [25]. For dimensions $d=2,\ 3$ comprehensive analytic solutions of the Hubbard and related models are not available. This is due to the complicated quantum dynamics and, in the case of fermions, the non-trivial algebra introduced by the Pauli exclusion principle.

In view of the fundamental limitations of exact analytical approaches one might hope that, at least, modern supercomputers can provide detailed numerical insights into the thermodynamic and spectral properties of correlated fermionic systems. However, classical computers are fundamentally limited by the exponential growth of the Hilbert space with system size. Therefore they can solve the Hubbard model and related correlation models only on finite, often rather small lattices and in certain parameter regimes (here "solving" means calculating the ground state energy and correlation functions, simulating dynamics and mapping out phase diagrams).[5] In principle, quantum computers will be able solve many-electron models much more efficiently than classical computers. However, there are still significant challenges. In particular, improve-

[4] More generally, the Hubbard model is the fundamental lattice model of quantum particles, since it may also be used for interacting bosons [20].

[5] Recently significant progress was made in the case of the three-dimensional Hubbard model at half-filling, where numerically exact auxiliary-field Quantum Monte Carlo computations of magnetic, thermodynamic, and dynamical properties have become possible for lattices up to 20^3 sites [26]. However, more complicated fermionic lattice models in $d=3$, especially models for realistic materials with many orbitals and energy bands, can be solved only on much smaller lattices.

ments in error correction, hardware scaling, and algorithm design will be necessary before it is possible to study large, realistic systems. Therefore quantum computers are not yet capable of accurately computing physical properties of large, realistic correlated electron systems beyond what classical methods can handle [27].
This shows very clearly that there is still a great need for analytically tractable, non-perturbative approximation schemes, which are applicable for all input parameters. Moreover, to understand the characteristic physical properties of a many-body problem "good" approximations are required.[6] Here mean-field theories play an important role.

3 Mean-field theories for the many-electron problem

In the theory of classical and quantum many-body systems an overall description of the properties of a model is often obtained within a *mean-field theory*. A mean-field theory is an approximation, where each particle (electron, spin, etc.) is assumed to experience an average ("mean") field created by all other particles, rather than the explicit particle-particle interaction. Although the term is frequently used it is not well defined, since there exist numerous ways to derive such theories. One construction scheme is based on the factorization of the interaction, as in the case of the mean-field theory for the Ising model for classical spins, or the Hartree-Fock theory for electronic models (see below). The factorization ("decoupling") implies a neglect of fluctuations (or of the correlation of fluctuations), which reduces the original many-body problem to a solvable "independent-particle" problem, where a single particle now interacts with a mean field provided by the other particles. Mean-field theories are a powerful first step for analyzing many-body systems; they provide qualitative insights and make calculations tractable.

3.1 Hartree-Fock theory

Hartree-Fock theory is an independent-electron approximation which, mathematically, may be interpreted in two different ways. Starting from the Hamiltonian level, it can be viewed as a factorization of the electron-electron interaction, whereby the actual many-electron problem is reduced to one where each electron now moves in a mean field (or mean potential) generated by all other electrons. This simplified problem is then solvable, the solution being given by the Hartree-Fock wave function, i.e., a single Slater determinant of one-electron spin-orbitals which ensures that the wave function remains antisymmetric under electron exchange, satisfying the Pauli exclusion principle. Alternatively, starting from the wave function, Hartree-Fock theory may be viewed as an approximation of the total N-electron wave function as a single Slater determinant of one-electron spin-orbitals. Applying this wave function to the electron-electron interaction corresponds to a decoupling of the interaction. Both views lead to the same results.

[6] Approximations are useful not only per se, but also because they allow us to better understand the key features of a complicated physics problem. As Peierls wrote: "*... the art of choosing a suitable approximation, of checking its consistency and finding at least intuitive reasons for expecting the approximation to be satisfactory, is much more subtle than that of solving an equation exactly*" [28].

While Hartree-Fock theory respects the Pauli principle, it neglects interaction-induced correlations between the electrons due to the decoupling/factorization procedure on which the approximation is based. Hence Hartree-Fock theory is a static mean-field approximation.[7]
To account for electronic correlation effects one must go beyond Hartree-Fock theory. Wigner [29] was apparently the first who tried to calculate the contribution of the mutual electronic interaction to the ground state energy beyond the Hartree-Fock result, which he referred to as "correlation energy". The correlation energy is defined as $E_{\text{corr}} = E_{\text{exact}} - E_{\text{HF}}$ where E_{exact} is the exact non-relativistic electronic energy and E_{HF} is the Hartree-Fock energy. Since Hartree-Fock theory does not include electron correlations, one always has $E_{\text{corr}} < 0$.

3.2 Infinite dimensions and mean-field behavior

Another, in general unrelated, mean-field construction scheme makes use of the simplifications that occur when some parameter is assumed to be large (in fact, infinite), whereby fluctuations are suppressed. In this case a particle no longer experiences the actual, fluctuating interaction with the other particles, but feels the interaction only as a "mean field". Depending on the model this parameter can be the length of the spins S, the spin degeneracy N, the spatial dimension d, or the coordination number Z, i.e., the number of nearest neighbors of a lattice site.[8], Mean-field theories obtained in such a limit, supplemented if possible by an expansion in the inverse of the large parameter, can provide valuable insights into the fundamental properties of a model. Perhaps the best-known mean-field theory in many-body physics is the "Weiss molecular-field theory" for the Ising model (see below). It is a prototypical "single-site mean-field theory" which becomes exact in the limit of infinite coordination number Z or infinite dimension d. It should be noted that the coordination number of a three-dimensional lattice can already be quite large, e.g., $Z = 6$ for a simple cubic lattice, $Z = 8$ for a bcc lattice and $Z = 12$ for an fcc-lattice.
Investigations of many-particle models in the limit $d, Z \to \infty$ do not go far back in time. In fact, Z was originally regarded as a measure of the *range* of the interaction between spins in the Ising

[7]The conclusion that Hartree-Fock theory does not include correlations calls for further discussion. The antisymmetry of the Hartree-Fock wave function required by the Pauli principle keeps electrons with equal spin apart, and thereby leads to a reduced probability of finding two electrons with the same spin close together in position space ("Pauli hole"). This corresponds to a spatial correlation, implying that Hartree-Fock theory *does* include a specific form of (static) correlation – at least for electrons with the same spin. However, this correlation is a result of the Fermi-Dirac statistics, i.e., is due to the effective quantum mechanical exchange interaction between indistinguishable electrons and is not caused by a classical force such as the Coulomb repulsion, which makes *all* electrons avoid each other ("Coulomb hole") regardless of spin to reduce the energy. The approximation of the many-electron wave function as a single Slater determinant means that each electron experiences an averaged potential rather than explicit electron-electron interactions. This neglects the instantaneous Coulomb interaction between electrons (i.e., the Hartree-Fock wave function does not adjust to the instantaneous repulsion), leading to an overestimation of the total energy. In particular, correlations among electrons with opposite spin are then completely missing. Therefore Hartree-Fock theory is a static mean-field approximation which does not describe (dynamic) electronic correlations between the electrons.

[8]For regular lattices both a dimension d and a coordination number Z can be defined. The coordination number Z is then determined by the dimension d and the lattice structure. But there exist other lattice-like structures, such as the Bethe lattice, which cannot be associated with a physical dimension d, although a coordination number Z is well-defined.

model, and thus of the number of spins in the range of the interaction [30]. In this case the limit $Z \to \infty$ describes an infinitely long-ranged interaction. Since a particle or spin then interacts with infinitely many other particles or spins (which are all "neighbors", i.e., the system has "infinite connectivity"), this limit was originally referred to as "limit of high density" [30] and only later as "limit of infinite dimensions" [31]. Thereafter the Ising model and other classical models were investigated on general d-dimensional hypercubic lattices. Today Z denotes the coordination number, i.e., the number of nearest neighbors.
Mean-field theories derived in the limit of infinite coordination number Z or dimension d provide an approximate solution of the many-body problem which retains characteristic features of the problem in $d < \infty$ and provides insights into the (unknown) solution in $d = 3$. This will now be illustrated by the Ising model in infinite dimensions.

3.2.1 Ising model

To explain ferromagnetism in three-dimensional solids from a microscopic point of view, Ising investigated a minimal model of interacting classical spins with a *non-magnetic* interaction between neighboring elementary magnets [32]. The Hamiltonian function for the Ising model with coupling J between two nearest-neighbor spins at lattice sites $\boldsymbol{R}_i$, $\boldsymbol{R}_j$ is given by

$$H = -\frac{1}{2} J \sum_{\langle \boldsymbol{R}_i, \boldsymbol{R}_j \rangle} S_i S_j, \tag{2}$$

where we assume ferromagnetic coupling ($J > 0$) and $\langle \boldsymbol{R}_i, \boldsymbol{R}_j \rangle$ indicates summation over all nearest-neighbor sites (the factor $1/2$ prevents double counting of sites). This can also be written as

$$H = -\sum_{\boldsymbol{R}_i} h_i S_i, \tag{3}$$

where now every spin S_i interacts with a site-dependent, i.e., locally fluctuating, field

$$h_i = J \sum_{\boldsymbol{R}_j}^{(i)} S_j \tag{4}$$

generated by the coupling of the spin S_i to its neighboring sites; here the superscript (i) on the summation symbol indicates summation over the Z nearest-neighbor sites of $\boldsymbol{R}_i$.

Mean field theory of the Ising model In mean-field theory the interaction of a spin with its local field in (3) is decoupled (factorized), i.e., h_i is replaced by a mean field h_{MF}, which leads to the mean-field Hamiltonian

$$H^{\mathrm{MF}} = -h_{\mathrm{MF}} \sum_{\boldsymbol{R}_i} S_i + E_{\mathrm{shift}} \,. \tag{5}$$

Now a spin S_i interacts only with a global field $h_{\mathrm{MF}} = JZS$ (the "molecular" or "Weiss" field), where $S \equiv \langle S_i \rangle = (1/L) \sum_{i=0}^{L} S_i$ is the average value of S_i, $E_{\mathrm{shift}} = LJZS^2/2$ is a constant energy shift, and L is the number of lattice sites of the system.

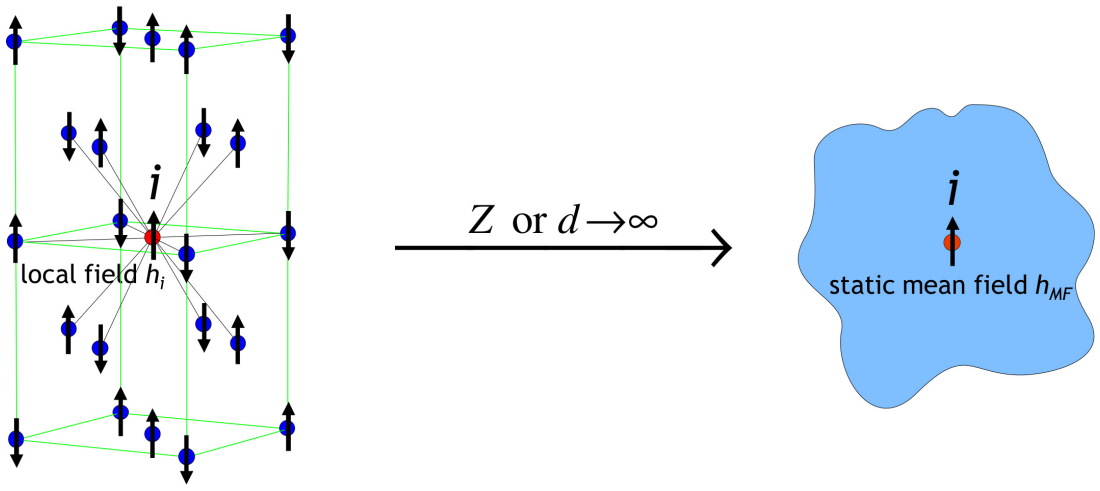

Fig. 2: *Already in three dimensions ($d = 3$) can the coordination number Z of a lattice be quite large, as in the face-centered cubic lattice shown on the left, where $Z = 12$. In the limit $Z \to \infty$, or equivalently $d \to \infty$, the Ising model effectively reduces to a single-site problem where the fluctuating local field h_i is replaced by a static global ("molecular") mean field $h_{\rm MF}$.*

Next we show that in infinite dimensions or for infinite coordination number Z this decoupling arises naturally. First we have to rescale the coupling constant J as

$$J = \frac{J^*}{Z} \ , \ J^* = \text{const.} \tag{6}$$

With this "classical scaling" $h_{\rm MF}$ and the energy (or the energy density in the thermodynamic limit) remain finite in the limit $Z \to \infty$. Writing $S_i = S + \delta S_i$, where δS_i is the deviation of S_i from its average S, (4) becomes $h_i = J^*\big(S + \Delta S_i\big)$, where

$$\Delta S_i = \frac{1}{Z} \sum_{\boldsymbol{R}_j}^{(i)} \delta S_j \tag{7}$$

is the sum of the fluctuations δS_j of the Z nearest-neighbor spins of S_i per nearest neighbor. These fluctuations are assumed to be uncorrelated, i.e., random. The law of large numbers then implies that the sum increases only as $\sqrt{Z}$ for $Z \to \infty$, such that ΔS_i altogether *decreases* as $1/\sqrt{Z}$ in this limit. As a consequence the local field h_i can indeed be replaced by its mean $h_{\rm MF}$ (central limit theorem). Hence the Hamiltonian function (5) becomes purely local

$$H^{\rm MF} = \sum_{\boldsymbol{R}_i} H_i + E_{\rm shift} \ , \tag{8}$$

where $H_i = -h_{\rm MF}\, S_i$. Thereby the problem reduces to an effective single-site problem (see Fig. 2). We note that S corresponds to the magnetization m of the system ($S \equiv m$). In the paramagnetic phase, where $m = 0$, the mean field $h_{\rm MF}$ vanishes; hence (5) and (8) are only non-trivial in the presence of ferromagnetic order.

The self-consistent equation of the mean-field theory The magnetization m is obtained from the partition function of the mean-field Hamiltonian (5) as $m = \tanh(\beta h_{\rm MF})$ where $\beta =$

$1/(k_BT)$. The condition $h_{\rm MF} = JZS \equiv J^*m$ then yields the well-known self-consistent equation for the magnetization m as

$$m = \tanh\big(\beta J^* m\big). \tag{9}$$

The mean-field theory is seen to become exact in the limit of infinite coordination number Z or dimension d.[9]
In this case $1/Z$ or $1/d$ serve as a small parameter which can be used, in principle, to improve the mean-field theory systematically (see section 7.1 of ref. [33]). This mean-field theory contains no unphysical singularities, is applicable for all values of the input parameters (temperature and/or external magnetic field) and is often viewed as the prototypical mean-field theory in statistical mechanics.

4 Static approximations for the Hubbard model

4.1 Factorization approach: Hartree mean-field theory

Lattice fermion models such as the Hubbard model are much more complicated than models with localized spins. Therefore the construction of a mean-field theory with the comprehensive properties of the mean-field theory of the Ising model will be more complicated, too. The simplest static mean-field theory of the Hubbard model is the Hartree approximation (an exchange (Fock) term does not arise in this case since the Hubbard interaction acts only for electrons with opposite spin on the same lattice site) [34]. To clarify the characteristic features of this mean-field theory we proceed as in the derivation of the mean-field theory of the Ising model and factorize the interaction term. To this end we rewrite the Hubbard interaction in the form of (3), i.e., we let an electron with spin σ at site $\boldsymbol{R}_i$ interact with a local field $\hat{h}_{i\sigma}$ ($\hat{h}_{i\sigma}$ is an operator and therefore a dynamic variable) produced by an electron with opposite spin on that site

$$\hat{H}_{\rm int} = \sum_{\boldsymbol{R}_i,\sigma} \hat{h}_{i\sigma}\hat{n}_{i\sigma}, \tag{10}$$

where $\hat{h}_{i\sigma} = \frac{1}{2}U\hat{n}_{i,-\sigma}$ (the factor $1/2$ is due to the summation over both spin directions). Next we replace the operator $\hat{h}_{i\sigma}$ by its expectation value $\langle\hat{h}_{i\sigma}\rangle$, now a real number, and obtain the single-particle ("mean-field") Hamiltonian

$$\hat{H}^{\rm MF} = \hat{H}_{\rm kin} + \sum_{\boldsymbol{R}_i,\sigma} \langle\hat{h}_{i\sigma}\rangle\hat{n}_{i\sigma} + E_{\rm shift}\,, \tag{11}$$

where $E_{\rm shift}$ is a constant energy shift. Now a σ-electron at site $\boldsymbol{R}_i$ interacts only with a local *static* field $\langle\hat{h}_{i\sigma}\rangle = \frac{1}{2}U\langle\hat{n}_{i-\sigma}\rangle$, which can be determined self-consistently using the single-particle Hamiltonian (11). The above decoupling of the operators corresponds to the Hartree approximation whereby correlated fluctuations *on* the site $\boldsymbol{R}_i$ are neglected.

[9] Due to the simplicity of the Ising model, the limits of infinite dimensions d and of infinitely long-ranged spin coupling J both yield the same mean-field theory. However, for more complicated models, in particular quantum models with itinerant degrees of freedom, this will generally not be the case.

It should be noted that although (11) is now an effective single-particle problem it can generally not be solved exactly since the mean field $\langle \hat{h}_{i\sigma} \rangle$ may vary from site to site, leading to solutions without long-range order. This is a new feature originating from the quantum-mechanical kinetic energy in the Hamiltonian.

The Hartree approximation is valid in the weak-coupling limit ($U \to 0$) and/or low-density limit ($n \to 0$), but clearly does not become exact in the limit $d \to \infty$, since the Hubbard interaction between two electrons is purely local and hence does not dependent on the spatial dimension. Therefore the physics behind the factorizations (8) and (11) is very different. Namely, (8) describes the decoupling of a spin from a bath of infinitely many neighboring spins whose fluctuations become unimportant in the limit $d \to \infty$, while (11) corresponds to the decoupling of an electron from *one* other electron (with opposite spin) on the same site.

While the Hartree approximation is useful for investigations at weak coupling, it will lead to fundamentally incorrect results at strong coupling when the double occupation of a lattice site becomes energetically very unfavorable and is therefore suppressed. Indeed, a factorization of the local correlation function $\langle \hat{n}_{i\uparrow} \hat{n}_{i\downarrow} \rangle \to \langle \hat{n}_{i\uparrow} \rangle \langle \hat{n}_{i\downarrow} \rangle$ eliminates correlation effects generated by the local quantum dynamics (see footnote 7). Hence the nature of the Hartree mean-field theory of spin-$\frac{1}{2}$ electrons with a local interaction is very different from the Weiss mean-field theory of spins with nearest-neighbor coupling.

4.2 Variational approach: Gutzwiller wave function

Another useful approximation scheme for quantum many-body systems makes use of variational wave functions [35]. Starting from a physically motivated many-body trial wave function the energy expectation value is calculated and is then minimized with respect to the variational parameters. Although variational wave functions usually yield only approximate results, they have several advantages: they are physically intuitive, can be custom tailored to a particular problem, can be used even when standard perturbation methods fail or are inapplicable, and provide a rigorous upper bound for the exact ground state energy by Ritz's variational principle.

To investigate the properties of the electronic correlation model (1) (which, actually, Gutzwiller was the first to introduce [17], but which was later named after Hubbard), Gutzwiller also proposed a simple variational wave function [17]. This "Gutzwiller wave function" introduces correlations into the ground-state wave function for non-interacting electrons through a correlation factor—a local operator in real space—which is constructed from the double occupation operator $\hat{D}$, (1c), as

$$|\Psi_G\rangle = g^{\hat{D}} |\mathrm{FG}\rangle = \prod_{\boldsymbol{R}_i} \left[1 - (1-g)\hat{D}_i\right] |\mathrm{FG}\rangle. \tag{12}$$

Here $|\mathrm{FG}\rangle$ is the wave function of the non-interacting Fermi gas and g is a variational parameter with $0 \leq g \leq 1$. The projector $g^{\hat{D}}$ globally reduces the amplitude of those spin configurations in $|\mathrm{FG}\rangle$ with too many doubly occupied sites for given repulsion U. The limit $g = 1$ describes the non-interacting case, while $g \to 0$ corresponds to $U \to \infty$.

The Gutzwiller wave function can be used to calculate the expectation value of an operator, e.g., the ground state energy of the Hubbard model, (1), as

$$E_{\rm G}(g,U) \equiv \frac{\langle \Psi_G|\hat{H}|\Psi_G\rangle}{\langle \Psi_G|\Psi_G\rangle}. \tag{13}$$

By computing the minimum of $E_{\rm G}(g,U)$ with respect to the variational parameter g, the latter is determined as a function of the interaction parameter U.

4.2.1 Gutzwiller approximation

In general the evaluation of expectation values in terms of $|\Psi_G\rangle$ cannot be performed exactly. Therefore Gutzwiller additionally introduced a non-perturbative approximation scheme whereby he obtained an explicit expression for the ground state energy of the Hubbard model [17, 36, 37]. The results of Gutzwiller's rather complicated approach were later re-derived by counting classical spin configurations [38] as described below; for details see ref. [39]. The idea behind the Gutzwiller approximation can be easily understood by calculating the norm $\langle \Psi_G|\Psi_G\rangle$. Namely, by working in configuration space the ground state of the Fermi gas can be written as

$$\big|{\rm FG}\big\rangle = \sum_D \sum_{\{i_D\}} A_{i_D} \big|\Psi_{i_D}\big\rangle, \tag{14}$$

where $|\Psi_{i_D}\rangle$ is a spin configuration with D doubly occupied sites, with A_{i_D} as the corresponding probability amplitude. The sum extends over the whole set $\{i_D\}$ of different configurations with the same D, and over all D. For a system with L lattice sites and N_σ electrons with spin σ ("σ-electrons") the number N_D of different configurations in $\{i_D\}$ is given by the combinatorial expression

$$N_D = \frac{L!}{L_\uparrow!\, L_\downarrow!\, D!\, E!}, \tag{15}$$

where $L_\sigma = N_\sigma - D$ and $E = L - N_\uparrow - N_\downarrow + D$ are the numbers of singly occupied and empty sites, respectively. Since $|\Psi_{i_D}\rangle$ is an eigenstate of $\hat{D}$, the norm of $|\Psi_G\rangle$ reads

$$\langle \Psi_G|\Psi_G\rangle = \sum_D g^{2D} \sum_{\{i_D\}} \big|A_{i_D}\big|^2. \tag{16}$$

The Gutzwiller approximation effectively amounts to neglecting spatial correlations between the spins of the electrons. The probability $|A_{i_D}|^2$ for a specific spin configuration with D doubly occupied sites is then the same for all configurations of electrons on the lattice, i.e., is given by the classical combinatorial result for uncorrelated particles

$$\big|A_{i_D}\big|^2 = P_\uparrow P_\downarrow\,. \tag{17}$$

Here $P_\sigma = 1/\binom{L}{N_\sigma} \simeq n_\sigma^{N_\sigma}(1-n_\sigma)^{L-N_\sigma}$, with $n_\sigma = N_\sigma/L$, is the probability for an arbitrary configuration of σ-electrons to occur. In this case (16) reduces to

$$\langle \Psi_G|\Psi_G\rangle = P_\uparrow P_\downarrow \sum_D g^{2D} N_D. \tag{18}$$

In the thermodynamic limit the sum in (18) is dominated by its largest term corresponding to a value $D = \bar{D}$, where $\bar{D}$ is determined by [36]

$$g^2 = \frac{\bar{d}\big(1 - n_\uparrow - n_\downarrow + \bar{d}\big)}{\big(n_\downarrow - \bar{d}\big)\big(n_\uparrow - \bar{d}\big)}, \tag{19}$$

with $\bar{d} = \bar{D}/L$. Equation (19) has the form of the law of mass action where, however, the correlation parameter g^2 rather than the Boltzmann factor regulates the dynamical equilibrium between the concentrations of singly occupied sites on one side of this "chemical reaction" and that of doubly occupied sites and holes on the other.[10] Eq. (19) uniquely relates $\bar{d}$ and g, such that g may be replaced by the quantity $\bar{d}$.

The expectation value of the interaction term, which is local in real space and thereby dimension independent, can be evaluated in the same way as $\langle \Psi_G | \Psi_G \rangle$. By contrast, the expectation value of the kinetic energy, which is non-local since it involves hopping between two sites, is approximated by neglecting the surrounding of these two sites, i.e., the two sites are thought to be decoupled from the rest of the system [39].

The non-magnetic ground state energy per lattice site of the Hubbard model at half filling ($n_\uparrow = n_\downarrow = 1/2$) is then found as

$$E_G[\bar{d}(g)]/L = q(\bar{d})\,\varepsilon_0 + U\,\bar{d}, \tag{20}$$

which has to be minimized with respect to the variational parameter $\bar{d}$. Here ε_0 is the internal energy of non-interacting electrons and $q = 8(1{-}2\bar{d})\bar{d} \leq 1$ may be viewed as a reduction factor of the kinetic energy (or the band width) due to correlations. In the Gutzwiller approximation, electronic correlations are therefore found to lead only to a simple renormalization of the kinetic energy of the electrons.

4.2.2 Brinkman-Rice metal-insulator transition

The results of the Gutzwiller approximation may be interpreted as follows [17, 36]: they describe a correlated, normal-state fermionic system at zero temperature whose momentum distribution has a discontinuity q at the Fermi level, where $q{=}1$ in the non-interacting case, which is reduced to $q < 1$ by the interaction as in a Landau Fermi liquid. In 1970 Brinkman and Rice [41] showed that for a half-filled band the minimization of (20) yields $q = 1{-}\bar{U}^2$, $\bar{d} = \frac{1}{4}\big(1{-}\bar{U}\big)$, and $E/L = -|\varepsilon_0|\big(1{-}\bar{U}\big)^2$, where $\bar{U} = U/\big(8|\varepsilon_0|\big)$. They noticed that in this case the Gutzwiller approximation describes a transition at a finite critical interaction strength $U_c = 8|\varepsilon_0|$ from an itinerant to a localized state, where lattice sites are singly occupied and the discontinuity q vanishes. This "Brinkman-Rice transition" therefore corresponds to a correlation induced ("Mott") metal-insulator transition. They argued [41] that the inverse of q can be identified with the effective mass of Landau quasiparticles, $q^{-1} = m^*/m \geq 1$, which diverges at U_c.

The results obtained with the Gutzwiller approximation are intuitively understandable (they are very "physical"). In the 1970s and 80s it was the only approximation scheme which was

[10] In fact, (19), with g^2 replaced by the Boltzmann factor $e^{-\beta U}$, is the exact result for the Hubbard model with infinite-range hopping [40].

able to describe a Mott metal-insulator transition at a finite value of the interaction *and* was in accord with basic properties of Landau Fermi liquid theory.[11] This was confirmed by a detailed investigation of the assumptions and implications of the Gutzwiller approximation that showed that the Gutzwiller-Brinkman-Rice theory was not only in qualitative [44], but even in good quantitative agreement with properties of normal-liquid ^{3}He [39]; for a discussion see section 3 of ref. [45].

4.2.3 Can the Gutzwiller approximation be derived by quantum many-body methods?

In the Gutzwiller approximation the quantum mechanical expectation value of the ground state energy of the Hubbard model is evaluated by counting classical spin configurations – hence it is a quasiclassical approximation [38, 39]. It was later shown that these results are reproduced by a two-site cluster factorization when intersite correlations are neglected [46]. Since intersite correlations decrease with increasing spatial dimension [46], it was to be expected that the Gutzwiller approximation is equivalent to a cluster expansion in position space in the limit $d \to \infty$ [39]. The question was then, whether the results of the Gutzwiller approximation – a real-space approximation for lattice fermions – can be derived also by quantum many-body theory in a systematic way.[12] A few years later Walter Metzner and I [49] provided an answer, by employing a new diagrammatic quantum many-body approach. Namely, we showed that the Gutzwiller approximation corresponds to the calculation of the expectation values of operators with the Gutzwiller wave function in the limit $d \to \infty$, as will be explained next; for a more detailed discussion see section 4 of ref. [45].

5 Lattice fermions in infinite dimensions

Using quantum many-body theory the expectation values of the kinetic and the interaction energy of the Hubbard model (1) in terms of the Gutzwiller wave function can be expressed diagrammatically for arbitrary dimensions d [49]. In $d = 1$ it is even possible to calculate and sum the diagrams analytically to all orders [49].[13] But this no longer works in dimensions $d = 2, 3$. By numerical calculations we found that in high dimensions the values of individual diagrams

[11] Other well-known approximation schemes, in particular those proposed by Hubbard, do not have these important properties: in the Hubbard-I approximation [18], which interpolates between the atomic limit and the non-interacting band, a band gap opens for any $U > 0$, while in the Hubbard-III approximation [42], which corresponds to the coherent potential approximation [43] for disordered systems, the Fermi surface volume is not conserved.

[12] I discussed this question in 1983-84 with several colleagues, in particular with Andrei Ruckenstein during my stay at the Bell Laboratories in Murray Hill in 1983. At that time Andrei tried to understand how to think about the Brinkman-Rice transition in correlated electronic systems in the presence of disorder. This eventually led him and Gabi Kotliar to formulate a functional integral representation of the Hubbard and Anderson models in terms of auxiliary bosons, whose simplest saddle-point approximation ("slave-boson mean-field theory") reproduces exactly the results of the Gutzwiller approximation [47,48]. Thus they had shown that the results of the Gutzwiller approximation could also be obtained without the use of the Gutzwiller variational wave function.

[13] The diagrams have the same form as the usual Feynman diagrams in quantum many-body theory, but a line corresponds to the time-independent single-particle density matrix $g^0_{ij,\sigma} = \langle \hat{c}^\dagger_{i\sigma} \hat{c}_{j\sigma} \rangle_0$ of the non-interacting system rather than to the single-particle propagator $G^0_{ij,\sigma}(t)$ since the variational approach involves only static quantities.

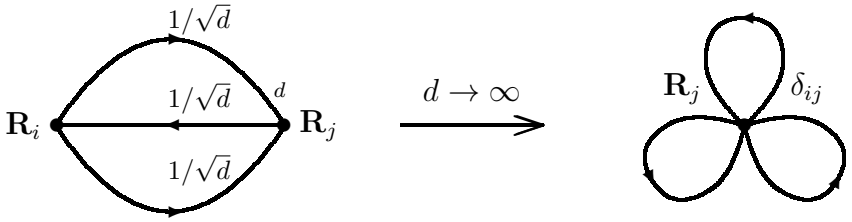

Fig. 3: *Collapse of the irreducible self-energy diagram for the Hubbard model in second-order perturbation theory in U in the limit $d \to \infty$. Left hand side: For nearest-neighbor sites $\boldsymbol{R}_i$, $\boldsymbol{R}_j$ the diagram is of the order $1/d^{3/2}$. Right hand side: Only for $i = j$ does the diagram give a finite contribution in the limit $d \to \infty$.*

approach a constant, which could be calculated analytically if the momentum conservation at a vertex was neglected. The sum over all diagrams gave exactly the results of the Gutzwiller approximation [49]. In view of the random generation of momenta in a typical Monte Carlo integration over momenta we concluded that the assumed independence of momenta at a vertex is correct in the limit of infinite spatial dimensions ($d \to \infty$). The results of the Gutzwiller approximation thus correspond to the evaluation of expectation values with the Gutzwiller wave function in the limit $d = \infty$. This immediately explained the quasiclassical nature of the Gutzwiller approximation. Most importantly, we had found that diagrammatic calculations in quantum many-body theory drastically simplify for $d \to \infty$. Clearly, the limit $d \to \infty$ was not only useful for the investigation of spin models, but also in the case of lattice fermion models.

5.1 Simplifications of diagrammatic quantum many-body theory

The simplifications of diagrammatic many-body theory for $d \to \infty$ are due to a collapse of irreducible diagrams in position space. This means that only site-diagonal ("local") diagrams (diagrams which only depend on a single site), remain [50, 51].[14] In particular, the irreducible self-energy is then completely local (Fig. 3).

To understand the reason for the diagrammatic collapse in $d \to \infty$ let us, for simplicity, consider diagrams where lines correspond to the single-particle density matrix $g^0_{ij,\sigma}$ as they enter in the calculation of expectation values with the Gutzwiller wave function (note that, since $g^0_{ij,\sigma} = \lim_{t\to 0^-} G^0_{ij,\sigma}(t)$, the following arguments are equally valid for the single-particle Green function $G^0_{ij,\sigma}(t)$ or its Fourier transform).

The single-particle density matrix $g^0_{ij,\sigma}$ may be interpreted as the quantum amplitude of the hopping of an electron with spin σ between sites $\boldsymbol{R}_i$ and $\boldsymbol{R}_j$. The square of its magnitude is therefore proportional to the *probability* of an electron to hop from $\boldsymbol{R}_j$ to a site $\boldsymbol{R}_i$. For nearest-neighbor sites $\boldsymbol{R}_i$, $\boldsymbol{R}_j$ on a lattice with coordination number Z this implies $|g^0_{ij,\sigma}|^2 \sim \mathcal{O}(1/Z)$,

[14] Gebhard later showed that in $d = \infty$ the calculation of expectation values with the Gutzwiller wave function can be performed even without diagrams [52]. This provided a direct link between the slave-boson mean-field theory and the results obtained with the Gutzwiller wave function in $d = \infty$. The latter approach was generalized by Gebhard and collaborators to multi-band Hubbard models, which can be used to describe the effect of correlations in real materials ("Gutzwiller density-functional theory") [53].

such that on a hypercubic lattice, where $Z = 2d$, and $d \to \infty$ one finds [50, 51]

$$g^0_{ij,\sigma} \sim \mathcal{O}\Big(\frac{1}{\sqrt{d}}\Big). \tag{21}$$

For general i, j one obtains [51, 54]

$$g^0_{ij,\sigma} \sim \mathcal{O}\Big(1/d^{\|\boldsymbol{R}_i - \boldsymbol{R}_j\|/2}\Big). \tag{22}$$

Here $\|\boldsymbol{R}\| = \sum_{n=1}^{d} |R_n|$ is the length of $\boldsymbol{R}$ in the "Manhattan metric", where electrons only hop along horizontal or vertical lines, but never along a diagonal; for further discussions of diagrammatic simplifications see ref. [55].

Consequences of the asymptotic d dependence of $g^0_{ij,\sigma}$ can be determined by examining the kinetic energy. For non-interacting electrons at $T = 0$ the expectation value of the kinetic energy is given by

$$E^0_{\rm kin} = -t \sum_{\langle \boldsymbol{R}_i, \boldsymbol{R}_j \rangle} \sum_{\sigma} g^0_{ij,\sigma}. \tag{23}$$

The sum over nearest neighbors leads to a factor $\mathcal{O}(Z)$ (which is $\mathcal{O}(d)$ for a hypercubic lattice). In view of the $1/\sqrt{d}$ dependence of $g^0_{ij,\sigma}$ for $d \to \infty$ it is therefore necessary to scale the nearest-neighbor hopping amplitude t as [50, 51]

$$t = \frac{t^*}{\sqrt{d}}, \; t^* = \text{const.}, \tag{24}$$

so that the kinetic energy remains finite for $d \to \infty$. The same result may be derived in a momentum-space formulation.[15] It is important to bear in mind that, although $g^0_{ij,\sigma}$ vanishes for $d \to \infty$, the electrons are still mobile. Indeed, even in the limit $d \to \infty$ the off-diagonal elements of $g^0_{ij,\sigma}$ contribute, since electrons may hop to $Z \sim \mathcal{O}(d)$ many nearest neighbors with amplitude $t^*/\sqrt{d}$.

5.2 The Hubbard model in $d = \infty$

A rescaling of the microscopic parameters of the Hubbard model with d is only required for the kinetic energy, since the interaction term is independent of the spatial dimension.[16] Altogether

[15] The need for the scaling (24) also follows from the density of states of non-interacting electrons. For nearest-neighbor hopping on a d-dimensional hypercubic lattice $\varepsilon_{\boldsymbol{k}}$ has the form $\varepsilon_{\boldsymbol{k}} = -2t \sum_{i=1}^{d} \cos k_i$ (here and in the following we set Planck's constant $\hbar$, Boltzmann's constant k_B, and the lattice spacing equal to unity). The density of states corresponding to $\varepsilon_{\boldsymbol{k}}$ is given by $N_d(\omega) = \sum_{\boldsymbol{k}} \delta(\omega - \varepsilon_{\boldsymbol{k}})$, which is the probability density for finding the value $\omega = \varepsilon_{\boldsymbol{k}}$ for a random choice of $\boldsymbol{k} = (k_1, \ldots, k_d)$. If the momenta k_i are chosen randomly, $\varepsilon_{\boldsymbol{k}}$ is the sum of d many independent (random) numbers $-2t \cos k_i$. The central limit theorem then implies that in the limit $d \to \infty$ the density of states is given by a Gaussian, i.e., $N_d(\omega) \stackrel{d\to\infty}{\longrightarrow} \frac{1}{2t\sqrt{\pi d}} \exp\Big[-\Big(\frac{\omega}{2t\sqrt{d}}\Big)^2\Big]$. Only if t is scaled with d as in (24) does one obtain a non-trivial density of states $N_\infty(\omega)$ in $d = \infty$ [56, 50] and thus a finite kinetic energy. The density of states on other types of lattices in $d = \infty$ can be calculated similarly [57, 58].

[16] Interactions beyond the Hubbard interaction, e.g., nearest-neighbor interactions such as $\hat{H}_{nn} = \sum_{\langle \boldsymbol{R}_i, \boldsymbol{R}_j \rangle} \sum_{\sigma\sigma'} V_{\sigma\sigma'} \hat{n}_{i\sigma} \hat{n}_{j\sigma'}$ have to be scaled, too, in the limit $d \to \infty$. In this case a scaling as in the Ising model, $V_{\sigma\sigma'} \to V^*_{\sigma\sigma'}/Z$, is required [59] ("classical scaling"). In $d = \infty$ non-local contributions therefore reduce to their (static) Hartree substitute and only the Hubbard interaction remains dynamical.

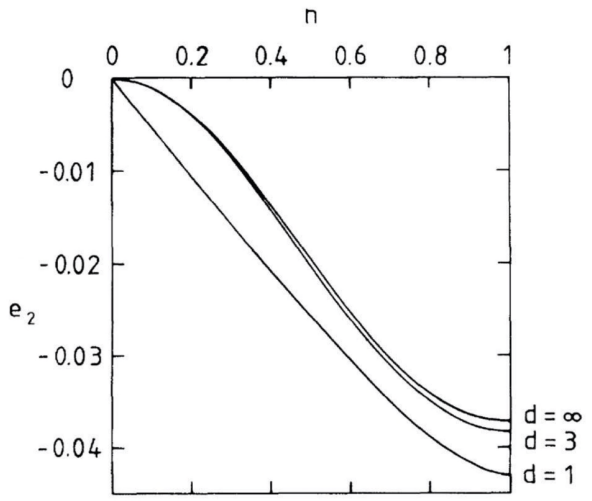

Fig. 4: *Correlation energy of the Hubbard model in second-order Goldstone perturbation theory in U in units of $2U^2/|\varepsilon_0|$ vs. density n in dimensions $d = 1, 3, \infty$. Here ε_0 is the kinetic energy for $U = 0$ and $n = 1$; adapted from ref. [50].*

this implies that only the Hubbard Hamiltonian with a rescaled kinetic energy

$$\hat{H} = -\frac{t^*}{\sqrt{d}} \sum_{\langle \boldsymbol{R}_i, \boldsymbol{R}_j \rangle} \sum_{\sigma} \hat{c}^\dagger_{i\sigma} \hat{c}_{j\sigma} + U \sum_{\boldsymbol{R}_i} \hat{n}_{i\uparrow} \hat{n}_{i\downarrow} \tag{25}$$

has a non-trivial $d \to \infty$ limit where both the kinetic energy and the interaction contribute (namely, it is the *competition* between the two terms which leads to interesting many-body physics). Therefore, even in $d = \infty$ the Hubbard model describes nontrivial correlations among the fermions. This is already evident in the evaluation of the second-order diagram in Goldstone perturbation theory for the correlation energy at weak coupling [50]. The integral over the three internal momenta (which, in $d = 3$, lead to nine integrals) reduces to a single integral in $d = \infty$. Obviously, calculations are much simpler in $d = \infty$ than in finite dimensions. More importantly, the results for the energy obtained in $d = \infty$ turn out to be very close to those in $d = 3$ (Fig. 4) and therefore provide a computationally simple, but quantitatively reliable approximation.

The simplifications in calculations for quantum lattice models such as the Hubbard model in infinite dimensions arise from the fact that energies are randomized by umklapp processes generated when lattice momenta are added [50]. Hence the energies become mutually independent, which allows one to replace the momentum integrations by energy integrations over the density of states. In other words, in $d = \infty$ the momentum conservation constraint at a vertex may be ignored.

With these results Walter and I had demonstrated [50] that microscopic calculations for correlated lattice fermions in $d = \infty$ dimensions were useful and very promising. Subsequently Müller-Hartmann [59] showed that in infinite dimensions the self-energy is $\boldsymbol{k}$-independent, i.e., local in position space, as in the Gutzwiller approximation, but remains dynamical

$$\Sigma_\sigma(\boldsymbol{k}, \omega) \overset{d\to\infty}{\equiv} \Sigma_\sigma(\omega), \tag{26}$$

whereby typical Fermi liquid features are preserved [60]. This result may be understood as follows [61, 62]: The influence of an interaction between particles on their motion is described quite generally by a complex, spatially dependent and dynamical field, the self-energy $\Sigma_\sigma(\boldsymbol{k},\omega)$. On a lattice with a very large number of nearest neighbors the *spatial* dependence of this field becomes increasingly unimportant and vanishes completely in $d=\infty$, as in the mean-field theory of the Ising model. So the field becomes a mean field in position space but retains its full dynamics.[17] Furthermore, Schweitzer and Czycholl [65] found that calculations for the periodic Anderson model also simplify in high dimensions, and Brandt and Mielsch [66] derived the exact solution of the Falicov-Kimball model in infinite dimensions by mapping the lattice problem onto a solvable atomic problem in a generalized, time-dependent external field; they also indicated that, in principle, such a mapping was even possible for the Hubbard model.[18]
Due to the $\boldsymbol{k}$-independence of the irreducible self-energy the most important obstacle for diagrammatic calculations in finite dimensions $d\geq 1$, namely the integration over intermediate momenta, is removed. At the same time the limit $d\to\infty$ does not affect the dynamics of the system. Hence, in spite of the simplifications in position or momentum space, the many-electron problem retains its full dynamics in $d=\infty$.

5.2.1 Single-particle propagator and spectral function

In $d=\infty$ the single-particle propagator of an interacting lattice fermion system (the "lattice Green function") at $T=0$ is then given by

$$G_{\boldsymbol{k},\sigma}(\omega)=\frac{1}{\omega-\varepsilon_{\boldsymbol{k}}+\mu-\Sigma_\sigma(\omega)}. \tag{27}$$

The $\boldsymbol{k}$-dependence of $G_{\boldsymbol{k}}(\omega)$ is now entirely due to the energy dispersion $\varepsilon_{\boldsymbol{k}}$ of the *non*-interacting particles. This means that in a homogeneous system described by the propagator

$$G_{ij,\sigma}(\omega)=L^{-1}\sum_{\boldsymbol{k}}G_{\boldsymbol{k},\sigma}(\omega)e^{i\boldsymbol{k}\cdot(\boldsymbol{R}_i-\boldsymbol{R}_j)} \tag{28}$$

its local part, $G_{ii,\sigma}\equiv G_\sigma$, is determined by

$$G_\sigma(\omega)=L^{-1}\sum_{\boldsymbol{k}}G_{\boldsymbol{k},\sigma}(\omega)=\int\limits_{-\infty}^{\infty}dE\,\frac{N_0(E)}{\omega-E+\mu-\Sigma_\sigma(\omega)}, \tag{29}$$

where $N_0(E)$ is the density of states of the non-interacting system. The spectral function of the interacting system (also often called density of states) is given by

$$A_\sigma(\omega)=-\frac{1}{\pi}\mathrm{Im}\,G_\sigma(\omega+i0^+). \tag{30}$$

[17] In this respect there is a direct analogy to non-interacting electrons in the present of static ("quenched") disorder, where the self-energy also becomes $\boldsymbol{k}$-independent in the limit $d\to\infty$ and plays the role of a coherent potential. The "coherent potential approximation" [43] is a single-site theory where an electron moves through an effective medium described by the self-energy $\Sigma_\sigma(\omega)$ that becomes exact in $d=\infty$ [61,63,64]. In the case of the Hubbard model in the limit $d\to\infty$ the coherent potential is much more complicated due to the explicit interaction between the particles (see footnote 21).

[18] Alternatively, it can be shown that in the limit $Z\to\infty$ the dynamics of the Falicov-Kimball model reduces to that of a non-interacting, tight-binding model on a Bethe lattice with coordination number $Z=3$ which can be solved analytically [67].

5.2.2 $\boldsymbol{k}$-independence of the self-energy and Fermi liquid behavior

The $\boldsymbol{k}$-independence of the self-energy allows one to make contact with Fermi liquid theory [60]. In general, i.e., even when Σ has a $\boldsymbol{k}$-dependence, the Fermi surface is defined by the $\omega = 0$ limit of the denominator of (27) (in the paramagnetic phase we can suppress the spin index)

$$\varepsilon_{\boldsymbol{k}} + \Sigma_{\boldsymbol{k}}(0) = E_F. \tag{31}$$

According to Luttinger and Ward [68] the volume within the Fermi surface is not changed by interactions, provided the latter can be treated in perturbation theory.[19] This is expressed by

$$n = \sum_{\boldsymbol{k}\sigma} \Theta\big(E_F - \varepsilon_{\boldsymbol{k}} - \Sigma_{\boldsymbol{k}}(0)\big), \tag{32}$$

where n is the electron density and $\Theta(x)$ is the step function. The $\boldsymbol{k}$-dependence of $\Sigma_{\boldsymbol{k}}(0)$ in (31) implies that, in spite of (32), the shape of the Fermi surface of the interacting system will be quite different from that of the non-interacting system, except for the rotationally invariant case $\varepsilon_{\boldsymbol{k}} = f(|\boldsymbol{k}|)$. By contrast, for lattice fermion models in $d = \infty$, where $\Sigma_{\boldsymbol{k}}(\omega) \equiv \Sigma(\omega)$, the Fermi surface itself, and hence the enclosed volume, is not changed by the interaction. The Fermi energy is simply shifted uniformly from its non-interacting value E_F^0 to $E_F = E_F^0 + \Sigma(0)$, to keep n in (32) constant. Thus $G(0)$, the $\omega = 0$ value of the local lattice Green function, and the spectral function $A(0) = -\frac{1}{\pi}\mathrm{Im}\, G(i0^+)$ are not changed by the interaction at all. This "pinning behavior" is well-known from the single-impurity Anderson model [70]. A renormalization of $N(0)$ can only be due to a $\boldsymbol{k}$-dependence of Σ.
For $\omega \to 0$ the self-energy has the property [60]

$$\mathrm{Im}\ \Sigma(\omega) \propto \omega^2, \tag{33}$$

which implies Fermi liquid behavior. The effective mass of the quasiparticles

$$\frac{m^*}{m} = 1 - \left.\frac{d\Sigma}{d\omega}\right|_{\omega=0} \tag{34}$$

$$= 1 + \frac{1}{\pi}\int_{-\infty}^{\infty} d\omega\, \frac{\mathrm{Im}\,\Sigma(\omega{+}i0^-)}{\omega^2} \geq 1 \tag{35}$$

is seen to be enhanced by the interaction. In particular, the momentum distribution

$$n_{\boldsymbol{k}} = \frac{1}{\pi}\int_{-\infty}^{0} d\omega\, \mathrm{Im}\, G_{\boldsymbol{k}}(\omega) \tag{36}$$

has a discontinuity at the Fermi surface given by $n_{k_F^-} - n_{k_F^+} = (m^*/m)^{-1}$, where $k_F^\pm = k_F \pm 0^+$.

[19] Recently, necessary and sufficient conditions for the validity of Luttinger's theorem [68] based on the Atiyah-Singer index theorem were derived, by which the topological robustness of a generalized Fermi surface may be quantified [69].

6 Dynamical mean-field theory for correlated electrons

The diagrammatic simplifications of quantum many-body theory for lattice fermions in $d = \infty$ provide the basis for the construction of a comprehensive mean-field theory of the Hubbard model which is diagrammatically controlled and whose free energy has no unphysical singularities. The construction is based on the scaled Hamiltonian (25). The self-energy is then momentum independent but retains its frequency dependence and thereby describes the full many-body dynamics of the interacting system. This is in contrast to Hartree(-Fock) theory where the self-energy acts only as a static potential. The resulting theory is both mean-field-like and dynamical and therefore represents a *dynamical* mean-field theory (DMFT) for lattice fermions which is able to describe genuine correlation effects as will be discussed in this section.

6.1 The self-consistent equations

In $d = \infty$ lattice fermion models with a local interaction effectively reduce to a single site embedded in a dynamical mean field provided by the other interacting fermions as illustrated in Fig. 5. The self-consistent DMFT equations can be derived in different ways depending on the physical interpretation of the correlation problem emerging in the limit $d, Z \to \infty$ [61, 71, 72]; for a discussion see ref. [55]. The mapping of the lattice electron problem onto a single-impurity Anderson model with a self-consistency condition in $d = \infty$ introduced by Georges and Kotliar [71], which was also employed by Jarrell [72], turned out to be the most useful approach,[20] since it made a connection with the well-studied theory of quantum impurities [70], for whose solution efficient numerical codes such as the quantum Monte Carlo (QMC) method [73] had already been developed and were readily available.[21] For a detailed discussion of the foundations of DMFT see the review by Georges, Kotliar, Krauth, and Rozenberg [74] and the lecture by Kollar at the Jülich Autumn School 2018 [75]; an introductory presentation can be found in ref. [76].

For $T > 0$ the self-consistent DMFT equations are given by:

(I) the *local propagator* $G_\sigma(i\omega_n)$, which is expressed by a functional integral as

$$G_\sigma(i\omega_n) = -\frac{1}{\mathcal{Z}} \int \prod_\sigma Dc_\sigma^* Dc_\sigma \, [c_\sigma(i\omega_n) c_\sigma^*(i\omega_n)] \, \exp[-S_{\rm loc}] \tag{37}$$

with the partition function

$$\mathcal{Z} = \int \prod_\sigma Dc_\sigma^* Dc_\sigma \, \exp[-S_{\rm loc}] \tag{38}$$

[20] The mapping itself can be performed without approximation, but leads to a complicated coupling between the impurity and the bath which makes the solution generally intractable. However, the problem can be solved in the limit $d \to \infty$ when the momentum dependence of the self-energy drops out.

[21] Alternatively, Janiš derived the self-consistent DMFT equations already in 1991 by generalizing the coherent potential approximation (CPA) [61]. In the CPA quenched disorder acting on non-interacting electrons is averaged and produces a mean field, the "coherent potential". In the case of the Hubbard model in $d = \infty$ the fluctuations generated by the Hubbard interaction may be treated as "annealed" disorder acting on non-interacting electrons [62] which, after averaging, produce a mean field, the self-energy. Numerical solutions of the DMFT equations starting from the CPA point of view have not been developed so far.

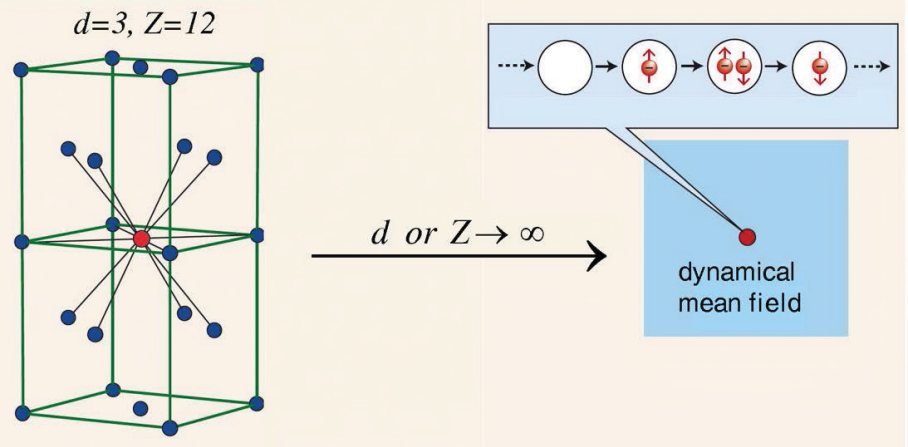

Fig. 5: *In the limit d or $Z \to \infty$ the Hubbard model effectively reduces to a dynamical single-site problem which may be viewed as a lattice site embedded in a $\boldsymbol{k}$-independent, dynamical fermionic mean field. Electrons can hop from the mean field onto this site and back, and interact on the site as in the original Hubbard model (see Fig.1). The local dynamics of the electrons is independent of the dimension or coordination number and therefore remains unchanged.*

and the local action

$$S_{\rm loc} \;=\; -\int_0^\beta d\tau_1 \int_0^\beta d\tau_2 \sum_\sigma c_\sigma^*(\tau_1)\, \mathcal{G}_\sigma^{-1}(\tau_1{-}\tau_2)\, c_\sigma(\tau_2) \;+\; U \int_0^\beta d\tau\, c_\uparrow^*(\tau) c_\uparrow(\tau) c_\downarrow^*(\tau) c_\downarrow(\tau). \quad (39)$$

Here $\mathcal{G}_\sigma$ is the effective local propagator (also called "bath Green function", or "Weiss mean field"[22]), which is defined by a Dyson equation

$$\mathcal{G}_\sigma(i\omega_n) = \big[[G_\sigma(i\omega_n)]^{-1} + \Sigma_\sigma(i\omega_n)\big]^{-1}. \quad (40)$$

Furthermore, by identifying the local propagator (37) with the Hilbert transform of the lattice Green function

$$G_{\boldsymbol{k}\,\sigma}(i\omega_n) = \frac{1}{i\omega_n - \varepsilon_{\boldsymbol{k}} + \mu - \Sigma_\sigma(i\omega_n)}, \quad (41)$$

(which is exact in $d = \infty$ [74]), one obtains
(II) the *self-consistency condition*

$$G_\sigma(i\omega_n) = \frac{1}{L}\sum_{\boldsymbol{k}} G_{\boldsymbol{k}\,\sigma}(i\omega_n) = \int_{-\infty}^{\infty} d\varepsilon\, \frac{N(\omega)}{i\omega_n - \varepsilon + \mu - \Sigma_\sigma(i\omega_n)} \quad (42)$$

$$= G_\sigma^0\big(i\omega_n{-}\Sigma_\sigma(i\omega_n)\big). \quad (43)$$

In (42) the ionic lattice enters only through the density of states of the non-interacting electrons. Eq. (43) illustrates the mean-field nature of the DMFT equations very clearly: the local Green function of the interacting system is given by the non-interacting Green function G_σ^0 at the shifted energy $i\omega_n{-}\Sigma_\sigma(i\omega_n)$, which is the energy measured relative to that of the surrounding fermionic bath, the dynamical mean field $\Sigma_\sigma(i\omega_n)$.

[22] This expresses the fact that $\mathcal{G}$ describes the coupling of a single site to the rest of the system, similar to the Weiss mean-field $h_{\rm MF}$ in the mean-field theory of the Ising model (see section 3.2.1). However, in the case of the DMFT the mean field depends on the frequency, i.e., is dynamical. It should be noted that, in principle, both local functions $\mathcal{G}_\sigma(i\omega_n)$ and $\Sigma_\sigma(i\omega_n)$ can be viewed as a dynamical mean field since both enter in the bilinear term of the local action (39).

6.1.1 Solving the self-consistent equations

The self-consistent DMFT equations can be solved iteratively: starting with an initial guess for the self-energy $\Sigma_\sigma(i\omega_n)$ one obtains the local propagator $G_\sigma(i\omega_n)$ from (42) and thereby the bath Green function $\mathcal{G}_\sigma(i\omega_n)$ from (40). This determines the local action (39) which is needed to compute a new value for the local propagator $G_\sigma(i\omega_n)$ from (37). By employing the old self-energy a new bath Green function $\mathcal{G}_\sigma$ is calculated and so on, until convergence is reached.

It should be stressed that although the DMFT corresponds to an effectively local problem, the propagator $G_{\boldsymbol{k}}(\omega)$ depends on the crystal momentum $\boldsymbol{k}$ through the dispersion relation $\varepsilon_{\boldsymbol{k}}$ of the non-interacting electrons. But there is no *additional* momentum-dependence through the self-energy, since this quantity is local within DMFT.

Solutions of the self-consistent DMFT equations require the extensive application of numerical methods, in particular quantum Monte Carlo (QMC) simulations [72, 74] with continuous-time QMC [77] still as the method of choice, the numerical renormalization group [78], the density matrix renormalization group [79], exact diagonalization [74], Lanczos procedures [80], and solvers based on matrix product states [81] or tensor networks [82]. Here the recent development of impurity solvers making use of machine learning [83] and quantum computers [84] open new perspectives.

6.2 Application of DMFT to the Hubbard model

In DMFT the mean field is dynamical, whereby local quantum fluctuations are fully taken into account, but is local (i.e., spatially independent) because of the infinitely many neighbors of every lattice site. The only approximation of this "single-site DMFT" when applied in $d < \infty$ is the neglect of the $\boldsymbol{k}$-dependence of the self-energy. DMFT provides a comprehensive, non-perturbative, thermodynamically consistent and diagrammatically controlled approximation scheme for the investigation of correlated lattice models at all interaction strengths, densities, and temperatures [74, 76], and can resolve even very low energy scales.

Intensive theoretical investigations of the Hubbard model and related correlation models using DMFT over the last three decades have provided a wealth of new insights into the physics described by this fundamental fermionic interaction model. In this subsection only a few exemplary results will be discussed; more detailed presentations can be found in refs. [74, 55], and the lecture notes of the Jülich Autumn Schools in 2011, 2014, 2018, and 2022 [12].

Most importantly, with DMFT it is possible to compute electronic correlation effects quantitatively in such a way that they can be tested experimentally, for example, by electron spectroscopies. Namely, DMFT describes the correlation induced transfer of spectral weight and the finite lifetime of quasiparticles through the real and imaginary part of the self-energy, respectively. This greatly helps to understand and characterize the Mott metal-insulator transition (MIT) to be discussed next.

6.2.1 Metal-insulator transitions

Mott-Hubbard transition The interaction-driven transition between a paramagnetic metal and a paramagnetic insulator, first discussed by Mott [85] and referred to as "Mott metal-insulator transition" (MIT), or "Mott-Hubbard MIT" when studied within the Hubbard model, is one of the most intriguing phenomena in condensed matter physics [86, 87]. This transition is a consequence of the quantum-mechanical competition between the kinetic energy of the electrons and their interaction U: the kinetic energy prefers the electrons to be mobile (a wave effect) which invariably leads to their interaction (a particle effect). For large values of U doubly occupied sites become energetically too costly. The system can reduce its total energy by localizing the electrons, which leads to a MIT. Here the DMFT provided detailed insights into the nature of the Mott-Hubbard-MIT for all values of the interaction U and temperature T [74, 88, 76, 55]. A microscopic investigation of the Mott MIT obtained within DMFT from a Fermi-liquid point of view was performed only recently [89].

While at small U the interacting system can be described by coherent quasiparticles whose spectral function ("density of states" (DOS)) still resembles that of the free electrons, the DOS in the Mott insulating state consists of two separate, incoherent "Hubbard bands" whose centers are separated approximately by the energy U (here we discuss only the half filled case without magnetic order). At intermediate values of U the spectrum then has a characteristic three-peak structure which is qualitatively similar to that of the single-impurity Anderson model [90] and which is a consequence of the three possible occupations of a lattice site: empty, singly occupied (up or down), and doubly occupied.

At $T = 0$ the width of the quasiparticle peak vanishes at a critical value of U which is of the order of the band width. So the Mott-Hubbard MIT occurs at intermediate coupling and therefore belongs to the hard problems in many-body theory, where most analytic approaches fail and investigations have to rely on numerical methods. Therefore several features of the Mott-Hubbard MIT near the transition point are still not sufficiently understood even within DMFT. Actually, it was recently argued that the Mott-Hubbard transition in the infinite-dimensional single-band Hubbard model may be understood as a topological phase transition, where the insulating state is the topological phase, and the transition from the metallic (Fermi liquid) to the insulating state involves domain wall dissociation [91].

At $T > 0$ the Mott-Hubbard MIT is found to be first order and is associated with a hysteresis region in the interaction range $U_{c1} < U < U_{c2}$ where U_{c1} and U_{c2} are the values at which the insulating and metallic solution, respectively, vanish [74, 88]; for more detailed discussions see refs. [74, 76, 55]. The hysteresis region terminates at a critical point, above which the transition becomes a smooth crossover from a "bad metal" to a "bad insulator"; for a schematic plot of the phase diagram see fig. 3 of ref. [76]. Transport in the incoherent region above the critical point shows remarkably rich properties, including scaling behavior [92]. The highly non-perturbative nature of the Mott MIT is illustrated by the fact that the MIT at $T = 0$ is an accumulation point of an infinite number of vertex divergence lines [93].

Mott-Hubbard MITs are found, for example, in transition metal oxides with partially filled

bands. For such systems band theory typically predicts metallic behavior. One of the most famous examples is V_2O_3 doped with Ti or Cr [94]. However, it is now known that certain organic materials are better realizations of the single-band Hubbard model without magnetic order and allow for more controlled investigations of the Mott MIT and the Mott state [95].

Metal-insulator transitions in the presence of disorder DMFT also provides a theoretical framework for the investigation of correlated electrons in the presence of disorder. In the absence of interactions, when the effect of local disorder is taken into account through the arithmetic mean of the local DOS (LDOS), DMFT is equivalent to the coherent potential approximation (CPA) [63, 64]; for a discussion see ref. [55]. However, CPA cannot describe Anderson localization. To overcome this deficiency a variant of the DMFT was formulated where the *geometrically* averaged LDOS is computed from the solutions of the self-consistent stochastic DMFT equations and is then fed into the self-consistency cycle [96]. This corresponds to a "typical medium theory" which is able to reproduce the Anderson transition of non-interacting electrons. By implementing this scheme into DMFT to study the properties of disordered electrons in the presence of interactions it is possible to compute the phase diagram of the Anderson-Hubbard model [97].

6.2.2 Metallic ferromagnetism

The Hubbard model was introduced in 1963 [17–19] in an attempt to explain metallic ferromagnetism in $3d$ metals such as Fe, Co, and Ni starting from a microscopic point of view. However, at that time investigations of the model employed severe, uncontrolled approximations. Therefore it was uncertain for a long time whether the Hubbard model can explain band ferromagnetism at realistic temperatures, electron densities, and interaction strengths in $d > 1$ at all. Using DMFT it was found that on generalized fcc-type lattices in $d = \infty$ (i.e., on "frustrated" lattices with large spectral weight at the lower band edge) the Hubbard model indeed predicts metallic ferromagnetic phases in large regions of the phase diagram [58, 98]. In the paramagnetic phase the susceptibility χ_F obeys a Curie-Weiss law [99], where the Curie temperature T_C is much lower than that obtained by Stoner theory, due to many-body effects. In the ferromagnetic phase the magnetization M is consistent with a Brillouin function as originally derived for localized spins, even for a *non-integer* magneton number as in $3d$ transition metals [58]. Therefore, DMFT accounts for the behavior of both the magnetization and the susceptibility of band ferromagnets [98]; see section 6.1 of my 2018 lecture notes [75]. Like the Mott MIT, metallic ferromagnetism is a hard intermediate-coupling many-electron problem.

6.2.3 Topological properties of correlated electron systems

The interest in non-trivial topological properties of electronic systems sparked by the theory of the quantum Hall effect, greatly increased when it was realized that the spin-orbit interaction can generate topologically insulating behavior [100]. Initially, investigations focused on topological features of non-interacting systems. But during the last decade the influence of

electronic interactions on these topological properties received more and more attention. Here DMFT turned out to be a useful tool. For example, DMFT was employed to study interaction effects in two-dimensional topological insulators [101], to analyze the robustness of the Chern number in the Haldane-Hubbard model [102], and to investigate the topological quantization of the Hall conductivity of correlated electrons at $T > 0$ [103]. Furthermore, to better understand the topological phase transition from a Weyl-semimetal to a Mott insulator the topological properties of quasiparticle bands were computed [104]. DMFT also made it possible to explore topological phase transitions in the Kitaev model in a magnetic field and to calculate the corresponding phase diagrams [105]. Correlation-induced topological effects can even arise from non-Hermitian properties of the single-particle spectrum in equilibrium systems [106]. Furthermore, it was demonstrated that a topologically nontrivial multiorbital Hubbard model remains well-defined and nontrivial in the limit $d \to \infty$ for arbitrary, but even, d [107]. Most recently, DMFT studies of the two-dimensional Hubbard model showed that correlated altermagnets can host Dirac points and topological phases [108].

6.2.4 Nonequilibrium DMFT

The study of correlated electrons out of equilibrium by employing a generalization of the DMFT has become another fascinating new research area [109]. Nonequilibrium DMFT is able to explain the results of time-resolved electron spectroscopy experiments, where femtosecond pulses are now available in a wide frequency range. In such experiments a probe is excited and the subsequent relaxation is studied. Thereby it was found, for example, that doubly occupied sites in the photo-excited quasi-2d transition-metal dichalcogenide 1T-TaS_2 show an ultrafast dynamics [110]. Such excitations may even result in long-lived, metastable ("hidden") states [111]. Quite generally, photo-induced nonequilibrium states in Mott insulators provide valuable information on correlation effects and metastable states of matter [112].

6.3 Beyond DMFT

Mean-field approximations provide useful information on the general physical properties of many-body problems. In particular, DMFT with its dynamical but local self-energy has been a breakthrough for the investigation and explanation of electronic correlation effects in models and materials. Although it is an approximation when used in $d < \infty$, experiments with cold atoms in optical lattices demonstrated that DMFT can be remarkably accurate in $d = 3$ [113]. A dynamical, local self-energy was also shown to be well justified in iron pnictides and chalcogenides [114] as well as in Sr_2RuO_4 [115]. Nevertheless mean-field results can neither explain correlation phenomena occurring on finite length scales or the critical behavior at thermal or quantum phase transitions, nor unconventional superconductivity observed in finite-dimensional systems. In such cases it is necessary to go beyond mean-field theory.

6.3.1 $1/d$ corrections

For mean-field theories derived in the limit $d \to \infty$ corrections can be obtained, at least in principle, by performing an expansion in the parameter $1/d$ around the mean-field results.[23]
An early strategy to include intersite quantum fluctuations into DMFT is "extended DMFT" (EDMFT) [116], where the interaction strength of a nearest-neighbor density-density interaction is scaled such that its fluctuation part contributes even in the large d limit.
Systematic calculations of $1/d$-corrections to the DMFT start with a Luttinger-Ward functional of the non-local Green function $G_{ij,\sigma}(i\omega_n)$, from which the non-local self-energy $\Sigma_{ij,\sigma}(i\omega_n)$ is obtained by functional derivative. To calculate first-order corrections in $1/d$ one needs to consider a pair of nearest-neighbor sites [117]. This generalizes the single-impurity problem of the DMFT to a two-impurity problem. It is then possible, in principle, to formulate a self-consistent, thermodynamically consistent approximation which is correct to order $1/d$ [117]. This scheme requires an exact cancellation of certain diagrams in the approximation. Unfortunately, numerical computations within this approach are unstable and can easily lead to acausal solutions. Although the scheme was modified such that the diagrammatic cancellation is assured at each iteration step [118] and thereby provided causal solutions in test calculations for the Hubbard model, acausal behavior cannot be ruled out in general. Therefore it is still not clear whether, and how, controlled and thermodynamically consistent $1/d$ expansions around DMFT can be constructed. So far, analytic calculations in this directions were not further pursued in view of the successes of numerical cluster approaches which, although not systematic in $1/d$, are explicitly causal [119] (see below).

6.3.2 Non-local extensions

There are different, mostly numerical, techniques to include non-local correlations into the DMFT; for a review see ref. [120]; in the following we mention three approaches:

Cluster extensions These methods incorporate short-range spatial correlations by solving an impurity problem for a cluster of sites rather than a single site. The dynamical cluster approximation (DCA) [121] systematically improves the accuracy by increasing the cluster size in momentum space, while the cellular DMFT (CDMFT) [122] works in real space. In both approaches the cluster is self-consistently embedded in a dynamical mean field. Thereby it has become possible to compute, for example, typical features of unconventional superconductivity in the Hubbard model in $d = 2$, such as the interplay of antiferromagnetism and d-wave pairing as well as pseudogap behavior [119], but also signatures of Anderson localization in disordered systems [123].

Diagrammatic generalizations By extending the DMFT on a diagrammatic level through the inclusion of non-local contributions, corrections to the local self-energy of the DMFT can

[23] For a discussion of the calculation of $1/d$ corrections to the Weiss mean-field theory of the Ising model, the Gutzwiller approximation, and the coherent potential approximation see section 7 of ref. [33].

be calculated explicitly. In particular, the dynamical vertex approximation (DΓA) [124] incorporates momentum-dependent vertex corrections beyond DMFT, while the dual fermion approach [125] introduces auxiliary fermions to capture long-range correlations. These approximations provided new insights into the mechanism of superconductivity arising from purely repulsive interactions, e.g., in the Kondo lattice [126] and Hubbard model [127]. In particular, in the Hubbard model a specific set of local particle-particle diagrams was identified which describe a strong screening of the bare interaction at low frequencies. Thereby antiferromagnetic spin fluctuations are suppressed, which in turn reduce the pairing interaction. Thus dynamical vertex corrections were found to lower T_c strongly [127]. With these approaches it is possible to determine critical behavior near thermal ($T > 0$) [128] and quantum phase transitions ($T = 0$) [129].

Functional renormalization group (fRG) The fRG method [130] systematically integrates out energy scales and captures collective fluctuations, which can be combined with DMFT to describe nonlocal correlations. In the DMF^{2}RG approach [131] the fRG flow does not start from the bare action of the system, but rather from the DMFT solution. Local correlations are thus included from the beginning, and nonlocal correlations are generated by the fRG flow, as demonstrated for the two-dimensional Hubbard model [131].

7 Understanding correlated materials with DMFT

It took several decades to develop theoretical techniques that made it possible to understand basic properties of the single-band Hubbard model. During this time first-principles investigations into the much more complicated many-body problem of correlated electron *materials* were out of reach. The electronic properties of solids were mainly studied within density-functional theory (DFT) [132], e.g., in the local density approximation (LDA) [133], the generalized gradient approximation (GGA) [134], and the LDA+U method [135]. Those approaches can describe the ground state properties of many simple elements and semiconductors, and even of some insulators, quite accurately, and often predict the magnetic and orbital properties [133] as well as the crystal structures of many solids correctly [136]. However, they fail to describe the electronic and structural properties of correlated paramagnetic materials since they miss characteristic features of correlated electron systems such as heavy quasiparticle behavior and Mott physics. DMFT changed this situation completely.

7.1 DFT+DMFT and GW+DMFT

The computational scheme introduced by Anisimov *et al.* [137] and Lichtenstein and Katsnelson [138], which merges material-specific DFT-based approximations with the many-body DMFT, provides a powerful new method for the microscopic computation of the electronic, magnetic, and structural properties of correlated materials from first principles even at finite temperatures [139–143]. This theoretical method is now often denoted by DFT+DMFT (or,

more specifically, LDA+DMFT, GGA+DMFT, etc.). In particular, this approach naturally accounts for the existence of local moments in the paramagnetic phase. By construction, DFT+DMFT includes the correct quasiparticle physics and the corresponding energetics, and reproduces the DFT results in the limit of weak Coulomb interaction U [144]. Most importantly, DFT+DMFT describes the correlation-induced many-body dynamics of strongly correlated electron materials at all values of the Coulomb interaction and doping.
As in the case of the single-band Hubbard model the many-body model of correlated materials constructed within the DFT+DMFT scheme consists of two parts: an effective kinetic energy obtained by DFT which describes the material-specific band structure of the uncorrelated electrons, and the local interactions between the electrons in the same orbital as well as in different orbitals. Here the static contribution of the electronic interactions already included in the DFT-approximations must be subtracted to avoid double counting [137–142]. Such a "double counting" correction is not necessary in the fully diagrammatic, but computationally very demanding GW+DMFT approach, where the LDA/GGA input is replaced by the GW approximation [145]. The resulting many-particle problem with its numerous energy bands and local interactions is then solved within DMFT, typically by CT-QMC.

7.2 Applications

7.2.1 Bulk materials

DFT+DMFT has been remarkably successful in the investigation of correlated materials, including transition metals and their oxides, manganites, fullerenes, Bechgaard salts, f-electron materials, magnetic superconductors, and Heusler alloys [139–142].
In particular, the application of DFT+DMFT led to the discovery of novel physical mechanisms and correlation phenomena. Take, for example, the Mott MIT. Within the single-band Hubbard model the Mott MIT was originally explained as a transition where the effective mass of quasiparticles diverges ("Brinkman-Rice scenario") [41]. When DMFT had made it possible to examine multi-band models, an orbitally-selective Mott MIT was identified [146]. Then, with the advent of DFT+DMFT, a site-selective Mott MIT was discovered in Fe_2O_3 with its numerous energy bands and local interactions [147].
In the following we illustrate the DFT+DMFT approach by its application to two paradigmatic materials, $SrVO_3$ and Fe.

$SrVO_3$: three-peak spectral function Transition metal oxides are an ideal laboratory for the study of electronic correlations in solids. Spectroscopic studies typically find a pronounced lower Hubbard band in the photoemission spectra which cannot be explained by conventional band-structure theory. $SrVO_3$ is a particularly simple correlated material due to its $3d^1$ configuration and its purely cubic crystal structure with one vanadium ion per unit cell. The cubic symmetry of the crystal field splits the fivefold degenerate $3d$ orbital into a threefold degenerate t_{2g} orbital and a twofold degenerate e_g orbital at higher energies. In the simplest approximation only the local interaction between the electrons in the t_{2g} orbitals is included. By employing

a variant of the LDA it is possible to compute the strength of the local Coulomb repulsion ($U \simeq 5.5$ eV) and the Hund's rule coupling ($J \simeq 1.0$ eV) [148]. Using these values the electronic band structure is calculated within LDA. The correlated electron problem defined in this way is solved numerically within DMFT. The spectral function shows the characteristic three-peak structure of a correlated metal (lower Hubbard band, quasiparticle peak, upper Hubbard band) [148, 149]. This was confirmed experimentally using electron spectroscopies [148, 150]. Recently it was pointed out that oxygen vacancy states created by UV or x-ray irradiation can strongly affect the line shapes of the lower Hubbard band and the quasiparticle peak [151], which must be taken into account in quantitative interpretations of those peaks.

Fe: electronic correlations and structural stability Iron (Fe) exhibits a rich phase diagram. Under ambient conditions Fe is ferromagnetic and has a bcc crystal structure (α phase). At the Curie temperature $T_C \sim 1043$ K the α phase becomes paramagnetic but retains its bcc structure. Only when the temperature is further increased to $T_{\text{struct}} \sim 1185$ K does a structural phase transition to a fcc structure (γ phase) take place. At $T \sim 1670$ K a transition to a second bcc structure (δ phase) occurs. DFT+DMFT calculations for ferromagnetic bcc Fe provide a semi-quantitative description of several physical properties of that phase (at least sufficiently far from the Curie point) and demonstrate that electronic correlations play an important role [152].[24] This approach also clarified the microscopic origin of the magnetic exchange interactions in the ferromagnetic phase [155]. While DFT band-structure methods provide qualitatively correct results for several electronic and structural properties of iron [156], their application in the case of the bcc-to-fcc phase transition predicts a simultaneous transition of the structural and the magnetic state. In fact, without magnetization standard band-structure methods find bcc iron to be unstable [157]. These discrepancies can been resolved by using DFT+DMFT to compute total energies [154, 158]. Thereby one obtains values of the lattice constant, unit cell volume, and bulk modulus of paramagnetic α iron which are in good quantitative agreement with experiment [154]. In particular, DFT+DMFT calculations of the equilibrium crystal structure and phase stability of iron find that the bcc-to-fcc phase transition indeed takes place at a temperature well above the magnetic transition (at about 1.3 T_C) and correctly determine the phonon dispersion and Debye temperature [154]. This approach is also of interest for geophysical studies, namely to explore iron and nickel at Earth's core conditions [159].

Furthermore, the study of Fe-based pnictides and chalcogenides led to the important insight that in metallic multi-orbital materials the intra-atomic exchange J can also induce strong correlations [160]. Clearly DMFT-based approaches will be very useful for the future design of correlated materials [161], such as materials with a high thermopower for thermoelectric devices which can convert waste heat into electric energy [162].

[24] In these investigations the lattice structure was assumed to be given and fixed. The question regarding the stability of the lattice structure in the presence of electronic correlations was studied, for example, in the case of plutonium [153] and iron at ambient pressure [154].

7.2.2 Surfaces, layers, and nanostructures

During the last few years DMFT investigations of inhomogeneous systems greatly improved our understanding of correlation effects at surfaces and interfaces, in thin films and multi-layered nanostructures [163], infinite layer nickelates [164], and twisted bilayer graphene [165]. This also opened new insights into potential functionalities of such structures and their application in electronic devices. DMFT has been extended to study correlations also in finite systems such as nanoscopic conductors and molecules [166]. In this way many-body effects were shown to be important even in biological matter [167].

8 Conclusions

The solution of the Hubbard model in $d = \infty$, which corresponds to a dynamical mean-field theory (DMFT) of correlated lattice fermions, has become the generic mean-field theory of correlated electrons. It provides a comprehensive, non-perturbative and thermodynamically consistent approximation scheme for the investigation of correlated fermions, especially electrons in solids and cold fermionic atoms in optical lattices, in finite dimensions. Non-local extensions of the DMFT now also allow to explain correlation effects which occur on the scale of several lattice constants and at thermal and quantum phase transitions. Most importantly, the combination of DMFT with methods for the computation of electronic band structures has led to a powerful new theoretical framework for the realistic study of correlated materials. The further development of this approach and its applications is the subject of current research.

References

[1] D.I. Khomskii: *Transition Metal Compounds* (Cambridge University Press, 2024)

[2] M.B. Maple, J. Phys. Soc. Jpn **74**, 222 (2005)

[3] D.M. Kennes, M. Claassen, L. Xian, A. Georges, A.J. Millis, J. Hone, C.R. Dean, D.N. Basov, A.N. Pasupathy, and A. Rubio, Nat. Phys. **17**, 155 (2021)

[4] N. Grewe and F. Steglich, in: K.A. Gschneidner Jr. and L. Eyring (eds.): *Handbook on the Physics and Chemistry of Rare Earths*, Vol. **14**, (North Holland, 1991), p. 343

[5] J.R. Schrieffer (ed.): *Handbook of High-Temperature Superconductivity* (Springer, 2007)

[6] E. Dagotto: *Nanoscale Phase Separation and Collossal Magnetoresistance* (Springer, 2002)

[7] M. Imada, A. Fujimori, and Y. Tokura, Rev. Mod. Phys. **70**, 1039 (1998)

[8] H.L. Stormer, D.C. Tsui, and A.C. Gossard, Rev. Mod. Phys. **71**, 298 (1999)

[9] H. v. Löhneysen, A. Rosch, M. Vojta, and P. Wölfle, Rev. Mod. Phys. **79**, 1015 (2007)

[10] Y. Tokura, Phys. Today **56**, No. 7, 50 (2003); E. Dagotto, Science **309**, 257 (2005)

[11] Z. Hennighausen and S. Kar, Electron. Struct. **3**, 014004 (2021)

[12] The Lecture Notes of the annual Jülich Autumn Schools on Correlated Electrons published by E. Pavarini, E. Koch and co-editors since 2011 provide extensive information on correlated electron systems and theoretical techniques for their investigation. [`https://www.cond-mat.de/events/correl.html`]

[13] W. Heisenberg, Z. Phys. **49**, 619 (1928)

[14] F. Bloch, Z. Phys. **57**, 545 (1929)

[15] L. Hoddeson, G. Baym, and M. Eckert, Rev. Mod. Phys. **59**, 287 (1987)

[16] D. Pines: *The Many-Body Problem* (W.A. Benjamin, Inc., Reading, 1962)

[17] M.C. Gutzwiller, Phys. Rev. Lett. **10**, 159 (1963)

[18] J. Hubbard, Proc. Roy. Soc. London A **276**, 238 (1963)

[19] J. Kanamori, Prog. Theor. Phys. **30**, 275 (1963)

[20] D. Jaksch, C. Bruder, J.I. Cirac, C.W. Gardiner, and P. Zoller, Phys. Rev. Lett. **81** 3108 (1998); I. Bloch, J. Dalibard, and W. Zwerger, Rev. Mod. Phys. **80**, 885 (2008)

[21] P.W. Anderson, Phys. Rev. **115**, 2 (1959)

[22] P.W. Anderson, Phys. Rev. **124**, 41 (1961)

[23] P.A. Wolff, Phys. Rev. **124**, 1030 (1961)

[24] M. Kollar, R. Strack, and D. Vollhardt, Phys. Rev. B **53**, 9225 (1996)

[25] E. Lieb and F.Y. Wu, Phys. Rev. Lett. **20**, 1445 (1968)

[26] Y.-F. Song, Y. Deng, Y.-Y. He, Phys. Rev. B **111**, 035123 (2025)

[27] S. Stanisic, J.L. Bosse, F.M. Gambetta, R.A. Santos, W. Mruczkiewicz, T.E. O'Brien, E. Ostby, and A. Montanaro, Nat. Commun. **13**, 5743 (2022);
A. Jafarizadeh, F. Pollmann, and A. Gammon-Smith, arXiv:2408.14543

[28] R. Peierls, Contemp. Phys. **21**, 3 (1980)

[29] E. Wigner, Phys. Rev. **46**, 1002 (1934)

[30] R. Brout, Phys. Rev. **118**, 1009 (1960)

[31] M.E. Fisher and D.S. Gaunt, Phys. Rev. **133**, A224 (1964)

[32] E. Ising, Z. Phys. **31**, 253 (1925)

[33] D. Vollhardt, in E. Pavarini, E. Koch, A. Lichtenstein, and D. Vollhardt (eds.): *Dynamical Mean-Field Theory of Correlated Electrons*, vol. 12 (Forschungszentrum Jülich, 2022) [https://www.cond-mat.de/events/correl22/manuscripts/]

[34] W. Langer, M. Plischke, and Mattis, Phys. Rev. Lett. **23**, 1448 (1969);
K. Dichtel, R.J. Jelitto, and H. Koppe, Z. Phys. **246**, 248 (1971)

[35] E. Feenberg: *Theory of Quantum Fluids* (Academic, New York, 1969);
V.R. Pandharipande and R.B. Wiringa, Rev. Mod. Phys. **51**, 821 (1979);
P. Fulde: *Electron Correlations in Molecules and Solids* (Springer, Berlin, 2002)

[36] M.C. Gutzwiller, Phys. Rev. **137**, A1726 (1965)

[37] P. Fazekas: *Lecture Notes on Electron Correlation and Magnetism* (World Scientific, Singapore, 1999)

[38] T. Ogawa, K. Kanda, and T. Matsubara, Prog. Theor. Phys. **53**, 614 (1975)

[39] D. Vollhardt, Rev. Mod. Phys. **56**, 99 (1984)

[40] P.G.J. van Dongen and D. Vollhardt, Phys. Rev. B **40**, 7252 (1989)

[41] W.F. Brinkman and T.M. Rice, Phys. Rev. B **2**, 4302 (1970)

[42] J. Hubbard, Proc. Roy. Soc. London A **281**, 401 (1964)

[43] R.J. Elliott, J.A. Krumhansl, and P.L. Leath, Rev. Mod. Phys. **46**, 465 (1974)

[44] P.W. Anderson and W.F. Brinkman, in K.H. Bennemann and J.B. Ketterson (eds.): *The Physics of Liquid and Solid Helium*, Part II, (Wiley, New York, 1978), p. 177

[45] D. Vollhardt, in E. Pavarini, E. Koch, D. Vollhardt, A. Lichtenstein (eds.): *DMFT at 25: Infinite Dimensions*, vol. 4 (Forschungszentrum Jülich, 2014) [https://www.cond-mat.de/events/correl14/manuscripts/]

[46] H.A. Razafimandimby, Z. Phys. B: Condens. Matter **49**, 33 (1982)

[47] For a personal account by Andrei Ruckenstein of the developments leading to the formulation of the Kotliar-Ruckenstein slave-boson mean-field theory see https://aspenphys.org/presidential-essay-from-andrei-ruckenstein/

[48] G. Kotliar and A.E. Ruckenstein, Phys. Rev. Lett. **57**, 1362 (1986)

[49] W. Metzner and D. Vollhardt, Phys. Rev. Lett. **59**, 121 (1987); W. Metzner and D. Vollhardt, Phys. Rev. B **37**, 7382 (1988); Erratum: *ibid.* **39**, 12339 (1989)

[50] W. Metzner and D. Vollhardt, Phys. Rev. Lett. **62**, 324 (1989)

[51] W. Metzner, Z. Phys. B: Condens. Matter **77**, 253 (1989)

[52] F. Gebhard, Phys. Rev. B **41**, 9452 (1990)

[53] J. Bünemann, F. Gebhard, and W. Weber, Found. Phys. **30**, 2011 (2000);
T. Schickling, J. Bünemann, F. Gebhard, and W. Weber, New J. Phys. **16**, 93034 (2014)

[54] P.G.J. van Dongen, F. Gebhard, D. Vollhardt, Z. Phys. B: Condens. Matter **76**, 199 (1989)

[55] D. Vollhardt, in A. Avella and F. Mancini (eds.): *Lectures on the Physics of Strongly Correlated Systems XIV*, *AIP Conference Proceedings*, vol. 1297, (American Institute of Physics, Melville, 2010), p. 339; [http://arxiv.org/abs/1004.5069v3]

[56] U. Wolff, Nucl. Phys. B **225**, 391 (1983)

[57] E. Müller-Hartmann, in E. Talik and J. Szade (eds.): *Proc. of the V. Symp. Phys. of Metals*, (Poland, 1991), p. 22; G.S. Uhrig, Phys. Rev. Lett. **77**, 3629 (1996)

[58] M. Ulmke, Euro. Phys. J. B **1**, 301 (1998)

[59] E. Müller-Hartmann, Z. Phys. B: Condens. Matter **74**, 507 (1989)

[60] E. Müller-Hartmann, Z. Phys. B: Condens. Matter **76**, 211 (1989)

[61] V. Janiš, Z. Phys. B: Condens. Matter **83**, 227 (1991)

[62] V. Janiš and D. Vollhardt, Int. J. Mod. Phys. **B6**, 731 (1992)

[63] R. Vlaming and D. Vollhardt, Phys. Rev. B **45**, 4637 (1992)

[64] V. Janiš and D. Vollhardt Phys. Rev. B **46**, 15712 (1992)

[65] H. Schweitzer and G. Czycholl, Solid State Commun. **69**, 171 (1989)

[66] U. Brandt and C. Mielsch, Z. Phys. B: Condens. Matter **75**, 365 (1989)

[67] P.G.J. van Dongen and D. Vollhardt, Phys. Rev. Lett. **65**, 1663 (1990)

[68] J.M. Luttinger and J.C. Ward, Phys. Rev. **118**, 1417 (1960);
J.M. Luttinger, Phys. Rev. **119**, 1153 (1960)

[69] J.T. Heath and K.S. Bedell, New J. Phys. **22** 063011 (2020)

[70] A.C. Hewson: *The Kondo Problem to Heavy Fermions* (Cambridge Univ. Press, 1997)

[71] A. Georges and G. Kotliar, Phys. Rev. B **45**, 6479 (1992)

[72] M. Jarrell, Phys. Rev. Lett. **69**, 168 (1992)

[73] J.E. Hirsch and R.M. Fye, Phys. Rev. Lett. **56**, 2521 (1986)

[74] A. Georges, G. Kotliar, W. Krauth, and M.J. Rozenberg, Rev. Mod. Phys. **68**, 13 (1996)

[75] E. Pavarini, E. Koch, A. Lichtenstein, and D. Vollhardt (eds.): *DMFT: From Infinite Dimensions to Real Materials*, vol. 8 (Forschungszentrum Jülich, 2018) [https://www.cond-mat.de/events/correl18/manuscripts/]

[76] G. Kotliar and D. Vollhardt, Phys. Today **57**, 53 (2004)

[77] E. Gull, A.J. Millis, A.I. Lichtenstein, A.N. Rubtsov, M. Troyer, P. Werner, Rev. Mod. Phys. **83**, 349 (2011)

[78] R. Bulla, T.A. Costi, and Th. Pruschke, Rev. Mod. Phys. **80**, 395 (2008)

[79] K. Hallberg, D.J. García, P.S. Cornaglia, J.I. Facio, and Y. Núñez-Fernández, EPL **112**, 17001 (2015)

[80] E. Koch, G. Sangiovanni, and O. Gunnarsson, Phys. Rev. B **78**, 115102 (2008); Y. Lu and M.W. Haverkort, Eur. Phys. J. Spec. Top. **226**, 2549 (2017)

[81] A. Holzner, A. Weichselbaum, and J. von Delft, Phys. Rev. B **81**, 125126 (2010); N.-O. Linden, M. Zingl, C. Hubig, O. Parcollet, and U. Schollwöck, Phys. Rev. B **101**, 041101(R) (2020)

[82] D. Bauernfeind, M. Zingl, R. Triebl, M. Aichhorn, and H.G. Evertz, Phys. Rev. X **7**, 031013 (2017)

[83] L.-F. Arsenault, A. Lopez-Bezanilla, O.A. von Lilienfeld, and A.J. Millis, Phys. Rev. B **90**, 155136 (2014); E. Sheridan, C. Rhodes, F. Jamet, I. Rungger, and C. Weber, Phys. Rev. B **104**, 205120 (2021)

[84] J. Selisko, M. Amsler, C. Wever, Y. Kawashima, G. Samsonidze, R. Ul Haq, F. Tacchino, I. Tavernelli, and T. Eckl, arXiv:2404.09527; C. Bertrand, P. Besserve, M. Ferrero, and T. Ayral, arXiv:2412.13711

[85] N.F. Mott, Proc. Phys. Soc. London, Ser. A **62**, 416 (1949); N.F. Mott, Rev. Mod. Phys. **40**, 677 (1968)

[86] N.F. Mott: *Metal-Insulator Transitions* (Taylor and Francis, London, 1990), 2nd edition

[87] M. Imada, A. Fujimori, and Y. Tokura, Rev. Mod. Phys. **70**, 1039 (1998)

[88] R. Bulla, Phys. Rev. Lett. **83**, 136 (1999); M.J. Rozenberg, R. Chitra, and G. Kotliar, Phys. Rev. Lett. **83**, 3498 (1999); J. Joo and V. Oudovenko, Phys. Rev. B **64**, 193102 (2001); R. Bulla, T.A. Costi, and D. Vollhardt, Phys. Rev. B **64**, 045103 (2001); N. Blümer: *Metal-Insulator Transition and Optical Conductivity in High Dimensions* (Shaker Verlag, Aachen, 2003)

[89] F. Krien, E.G.C.P. van Loon, M.I. Katsnelson, A.I. Lichtenstein, and M. Capone, Phys. Rev. B **99**, 245128 (2019)

[90] O. Gunnarsson and K. Schönhammer, Phys. Rev. B **31**, 4815 (1985); R. Bulla, A.C. Hewson, and Th. Pruschke, J. Phys.: Condens. Matter **10**, 8365 (1998)

[91] S. Sen, P.J. Wong, and A.K. Mitchell, Phys. Rev. B **102**, 081110 (2020)

[92] H. Terletska, J. Vučičević, D. Tanasković, and V. Dobrosavljević, Phys. Rev. Lett. **107**, 026401 (2011); J. Vučičević, H. Terletska, D. Tanasković, and V. Dobrosavljević, Phys. Rev. B **88**, 075143 (2013)

[93] M. Pelz, S. Adler, M. Reitner, A. Toschi, Phys. Rev. B **108** 155101 (2023)

[94] D.B. McWhan, A. Menth, J.P. Remeika, W.F. Brinkman, T.M. Rice, Phys. Rev. B **7**, 1920 (1973); P. Limelette, A. Georges, D. Jerome, P. Wzietek, P. Metcalf, J.M. Honig, Science **302**, 89 (2003); P. Hansmann, A. Toschi, G. Sangiovanni, T. Saha-Dasgupta, S. Lupi, M. Marsi, K. Held, Phys. Status Solidi B **250**, 1251 (2013); J.C. Leiner, H.O. Jeschke, R. Valentí, S. Zhang, A.T. Savici, J.Y.Y. Lin, M.B. Stone, M.D. Lumsden, Jiawang Hong, O. Delaire, Wei Bao, C.L. Broholm, Phys. Rev. X **9**, 011035 (2019)

[95] P. Limelette, P. Wzietek, S. Florens, A. Georges, T.A. Costi, C. Pasquier, D. Jérome, C. Mézière, and P. Batail, Phys. Rev. Lett. **91**, 016401 (2003); F. Kagawa, T. Itou, K. Miyagawa, and K. Kanoda, Phys. Rev. B **69**, 064511 (2004); A. Pustogow, Y. Saito, A. Löhle, M.S. Alonso, A. Kawamoto, V. Dobrosavljević, M. Dressel, and S. Fratini, Nat. Commun. **12**, 1571 (2021)

[96] V. Dobrosavljević and G. Kotliar, Phys. Rev. Lett. **78**, 3943 (1997); V. Dobrosavljević, A.A. Pastor, and B.K. Nikolić, Europhys. Lett. **62**, 76 (2003); S. Mahmoudian, S. Tang, and V. Dobrosavljević, Phys. Rev. B **92**, 144202 (2015)

[97] K. Byczuk, W. Hofstetter, and D. Vollhardt, Phys. Rev. Lett. **94**, 056404 (2005); *ibid.* **102**, 146403 (2009); K. Byczuk, W. Hofstetter, and D. Vollhardt, in E. Abrahams (ed.): *Fifty Years of Anderson Localization* (World Scientific, Singapore, 2010), p. 473 [reprinted in Int. J. Mod. Phys. B **24**, 1727 (2010)]

[98] D. Vollhardt, N. Blümer, K. Held, and M. Kollar, Lecture Notes in Physics **580**, 191 (Springer, Heidelberg, 2001)

[99] K. Byczuk and D. Vollhardt, Phys. Rev. B **65**, 134433 (2002)

[100] M.Z. Hasan and C.L. Kane, Rev. Mod. Phys. **82**, 3045 (2010)

[101] Y. Tada, R. Peters, M. Oshikawa, A. Koga, N. Kawakami, and S. Fujimoto, Phys. Rev. B **85**, 165138 (2012)

[102] T. Mertz, K. Zantout, and R. Valentí, Phys. Rev. B **100**, 125111 (2019)

[103] A.A. Markov, G. Rohringer, and A.N. Rubtsov, Phys. Rev. B **100**, 115102 (2019)

[104] B. Irsigler, T. Grass, J.-H. Zheng, M. Barbier, and W. Hofstetter, Phys. Rev. B **103**, 125132 (2021)

[105] S. Liang, M.-H. Jiang, W. Chen, J.-X. Li, and Q.-H. Wang, Phys. Rev. B **98**, 054433 (2018)

[106] T. Yoshida, R. Peters, and N. Kawakami, Phys. Rev. B **98**, 035141 (2018); Y. Nagai, Y. Qi, H. Isobe, V. Kozii, L. Fu, Phys. Rev. Lett. **125**, 227204 (2020)

[107] D. Krüger and M. Potthoff, Phys. Rev. Lett. **126**, 196401 (2021)

[108] L. Del Re, arXiv:2408.14288

[109] H. Aoki, N. Tsuji, M. Eckstein, M. Kollar, T. Oka, and P. Werner, Rev. Mod. Phys. **86**, 779 (2014)

[110] M. Ligges, I. Avigo, D. Golež, H.U.R. Strand, Y. Beyazit, K. Hanff, F. Diekmann, L. Stojchevska, M. Kalläne, P. Zhou, K. Rossnagel, M. Eckstein, P. Werner, and U. Bovensiepen, Phys. Rev. Lett. **120**, 166401 (2018); Erratum: *ibid.* **122**, 159901 (2019)

[111] J. Li, H.U.R. Strand, P. Werner, and M. Eckstein, Nat. Commun. **9**, 4581 (2018)

[112] Y. Murakami, D. Golež, M. Eckstein, and P. Werner, arXiv:2310.05201

[113] U. Schneider, L. Hackermüller, S. Will, Th. Best, I. Bloch, T.A. Costi, R.W. Helmes, D. Rasch, A. Rosch, Science **322**, 1520 (2008)

[114] P. Sémon, K. Haule, and G. Kotliar, Phys. Rev. B **95**, 195115 (2017)

[115] A. Tamai, M. Zingl, E. Rozbicki, E. Cappelli, S. Riccò, A. de la Torre, S. McKeown Walker, F.Y. Bruno, P.D.C. King, W. Meevasana, M. Shi, M. Radović, N.C. Plumb, A.S. Gibbs, A.P. Mackenzie, C. Berthod, H. Strand, M. Kim, A. Georges, and F. Baumberger, Phys. Rev. X **9**, 021048 (2019)

[116] Q. Si and J.L. Smith (1996), Phys. Rev. Lett. **77**, 3391 (1996); J.L. Smith and Q. Si, Phys. Rev. B **61**, 5184 (2000); R. Chitra and G. Kotliar, Phys. Rev. Lett. **84**, 3678 (2000); P. Sun and G. Kotliar, Phys. Rev. B **66**, 085120 (2002)

[117] A. Schiller and K. Ingersent, Phys. Rev. Lett. **75**, 113 (1995)

[118] G. Zaránd, D.L. Cox, and A. Schiller, Phys. Rev. B **62**, R16227 (2000)

[119] Th. Maier, M. Jarrell, Th. Pruschke, and M.H. Hettler, Rev. Mod. Phys. **77**, 1027 (2005)

[120] G. Rohringer, H. Hafermann, A. Toschi, A.A. Katanin, A.E. Antipov, M.I. Katsnelson, A.I. Lichtenstein, A.N. Rubtsov, and K. Held, Rev. Mod. Phys. **90**, 025003 (2018)

[121] M.H. Hettler, A.N. Tahvildar-Zadeh, M. Jarrell, Th. Pruschke, and H.R. Krishnamurthy, Phys. Rev. B **58**, R7475 (1998)

[122] A.I. Lichtenstein, and M.I. Katsnelson, Phys. Rev. B **62**, R9283 (2000); G. Kotliar, S.Y. Savrasov, G. Pálsson, and G. Biroli, Phys. Rev. Lett. **87**, 186401 (2001)

[123] C.E. Ekuma, H. Terletska, K.-M. Tam, Z.-Y. Meng, J. Moreno, and M. Jarrell, Phys. Rev. B **89**, 081107(R) (2014); H. Terletska, Y. Zhang, K.M. Tam, T. Berlijn, L. Chioncel, N.S. Vidhyadhiraja, and M. Jarrell, Appl. Sci. **8**, 2401 (2018)

[124] A. Toschi, A.A. Katanin, and K. Held, Phys Rev. B **75**, 045118 (2007)

[125] A.N. Rubtsov, M.I. Katsnelson, and A.I. Lichtenstein, Phys. Rev. B **77**, 033101 (2008)

[126] J. Otsuki, Phys. Rev. Lett. **115**, 036404 (2015)

[127] M. Kitatani, T. Schäfer, H. Aoki, and K. Held, Phys Rev. B **99**, 041115(R) (2019)

[128] T. Schäfer, A.A. Katanin, K. Held, and A. Toschi, Phys. Rev. Lett. **119**, 046402 (2017)

[129] D. Hirschmeier, H. Hafermann, and A.I. Lichtenstein, Phys. Rev. B **97**, 115150 (2018); T. Schäfer, A.A. Katanin, M. Kitatani, A. Toschi, and K. Held, Phys. Rev. Lett. **122**, 227201 (2019)

[130] W. Metzner, M. Salmhofer, C. Honerkamp, V. Meden, and K. Schönhammer, Rev. Mod. Phys. **84**, 299 (2012)

[131] C. Taranto, S. Andergassen, J. Bauer, K. Held, A. Katanin, W. Metzner, G. Rohringer, and A. Toschi, Phys. Rev. Lett. **112**, 196402 (2014); D. Vilardi, C. Taranto, and W. Metzner, Phys. Rev. B **99**, 104501 (2019)

[132] P. Hohenberg and W. Kohn, Phys. Rev. B **136**, 864 (1964); W. Kohn and L.J. Sham, Phys. Rev. **140**, A1133 (1965)

[133] R.O. Jones and O. Gunnarsson, Rev. Mod. Phys. **61**, 689 (1989)

[134] J.P. Perdew, K. Burke, and M. Ernzerhof, Phys. Rev. Lett. **77**, 3865 (1996)

[135] V.I. Anisimov, J. Zaanen, and O.K. Andersen, Phys. Rev. B **44**, 943 (1991)

[136] S. Baroni, S. de Gironcoli, A.D. Corso, and P. Giannozzi, Rev. Mod. Phys. **73**, 515 (2001)

[137] V.I. Anisimov, A.I. Poteryaev, M.A. Korotin, A.O. Anokhin, and G. Kotliar, J. Phys.: Condens. Matter **9**, 7359 (1997)

[138] A.I. Lichtenstein and M.I. Katsnelson, Phys. Rev. B **57**, 6884 (1998)

[139] K. Held, I.A. Nekrasov, G. Keller, V. Eyert, N. Blümer, A.K. McMahan, R.T. Scalettar, Th. Pruschke, V.I. Anisimov, and D. Vollhardt, Psi-k Newsletter **56**, 65 (2003) [reprinted in Phys. Status Solidi B **243**, 2599 (2006)]; K. Held, Adv. Phys. **56**, 829 (2007)

[140] G. Kotliar, S.Y. Savrasov, K. Haule, V.S. Oudovenko, O. Parcollet, and C.A. Marianetti, Rev. Mod. Phys. **78**, 865 (2006)

[141] M.I. Katsnelson, V. Yu. Irkhin, L. Chioncel, A.I. Lichtenstein, and R.A. de Groot, Rev. Mod. Phys. **80**, 315 (2008)

[142] D. Vollhardt and A.I. Lichtenstein (eds.): *Dynamical Mean-Field Approach with Predictive Power for Strongly Correlated Materials*, Eur. Phys. J. Spec. Top. **226** (2017)

[143] D. Vollhardt, JPS Conf. Proc. **30**, 011001 (2020)

[144] A. Carta, I. Timrov, P. Mlkvik, A. Hampel, C. Ederer, arXiv:2411.03937

[145] S. Biermann, F. Aryasetiawan, and A. Georges, Phys. Rev. Lett. **90**, 086402 (2003); S. Biermann, J. Phys.: Condens. Matter **26**, 173202 (2014); J.M. Tomczak, P. Liu, A. Toschi, G. Kresse, and K. Held, Eur. Phys. J. Spec. Top. **226**, 2565 (2017)

[146] L. de'Medici, A. Georges, and S. Biermann, Phys. Rev. B **72**, 205124 (2005)

[147] E. Greenberg, I. Leonov, S. Layek, Z. Konopkova, M.P. Pasternak, L. Dubrovinsky, R. Jeanloz, I.A. Abrikosov, and G. Kh. Rozenberg, Phys. Rev. X **8**, 031059 (2018)

[148] A. Sekiyama, H. Fujiwara, S. Imada, S. Suga, H. Eisaki, S.I. Uchida, K. Takegahara, H. Harima, Y. Saitoh, I.A. Nekrasov, G. Keller, D.E. Kondakov, A.V. Kozhevnikov, Th. Pruschke, K. Held, D. Vollhardt, and V.I. Anisimov, Phys. Rev. Lett. **93**, 156402 (2004); I.A. Nekrasov, G. Keller, D.E. Kondakov, A.V. Kozhevnikov, Th. Pruschke, K. Held, D. Vollhardt, and V.I. Anisimov, Phys. Rev. B **72**, 155106 (2005); I.A. Nekrasov, K. Held, G. Keller, D.E. Kondakov, Th. Pruschke, M. Kollar, O.K. Andersen, V.I. Anisimov, and D. Vollhardt, Phys. Rev. B **73**, 155112 (2006)

[149] E. Pavarini, S. Biermann, A. Poteryaev, A.I. Lichtenstein, A. Georges, and O.K. Andersen, Phys. Rev. Lett. **92**, 176403 (2004)

[150] I.H. Inoue, I. Hase, Y. Aiura, A. Fujimori, K. Morikawa, T. Mizokawa, Y. Haruyama, T. Maruyama, and Y. Nishihara, Physica C **235-240**, 1007 (1994)

[151] M. Sing, H.O. Jeschke, F. Lechermann, Valentí, and R. Claessen, Eur. Phys. J. Spec. Top. **226**, 2457 (2017)

[152] A.I. Lichtenstein, M.I. Katsnelson, and G. Kotliar, Phys. Rev. Lett. **87**, 067205 (2001); J. Sánchez-Barriga, J. Fink, V. Boni, I. Di Marco, J. Braun, J. Minár, A. Varykhalov, O. Rader, V. Bellini, F. Manghi, H. Ebert, M.I. Katsnelson, A.I. Lichtenstein, O. Eriksson, W. Eberhardt, and H.A. Dürr, Phys. Rev. Lett. **103**, 267203 (2009)

[153] X. Dai, S.Y. Savrasov, G. Kotliar, A. Migliori, H. Ledbetter, and E. Abrahams, Science **300**, 953 (2003)

[154] I. Leonov, A.I. Poteryaev, V.I. Anisimov, and D. Vollhardt, Phys. Rev. Lett. **106**, 106405 (2011); I. Leonov, A.I. Poteryaev, V.I. Anisimov, and D. Vollhardt, Phys. Rev. B **85**, R020401 (2012); I. Leonov, A.I. Poteryaev, Y.N. Gornostyrev, A.I. Lichtenstein, M.I. Katsnelson, V.I. Anisimov, and D. Vollhardt, Sci. Rep. **4**, 5585 (2014); J. Kuneš, I. Leonov, P. Augustinský, V. Křápek, M. Kollar, and D. Vollhardt, Eur. Phys. J. Spec. Top. **226**, 2641 (2017)

[155] Y.O. Kvashnin, R. Cardias, A. Szilva, I. Di Marco, M.I. Katsnelson, A.I. Lichtenstein, L. Nordström, A.B. Klautau, and O. Eriksson, Phys. Rev. Lett. **116**, 217202 (2016);

A.A. Katanin, A.S. Belozerov, A.I. Lichtenstein, and M.I. Katsnelson, Phys. Rev. B **107**, 235118 (2023)

[156] D.J. Singh, W.E. Pickett, and H. Krakauer, Phys. Rev. B **43**, 11628 (1991); S.V. Okatov, A.R. Kuznetsov, Y.N. Gornostyrev, V.N. Urtsev, and M.I. Katsnelson, Phys. Rev. B **79**, 094111 (2009);

[157] H.C. Hsueh, J. Crain, G.Y. Guo, H.Y. Chen, C.C. Lee, K.P. Chang, and H.L. Shih, Phys. Rev. B **66**, 052420 (2002)

[158] H. Park, A.J. Millis, and C.A. Marianetti, Phys. Rev. B **90**, 235103 (2014)

[159] A. Hausoel, M. Karolak, E. Şaşıoğlu, A. Lichtenstein, K. Held, A. Katanin, A. Toschi, and G. Sangiovanni, Nat. Commun. **8**, 16062 (2017); L.V. Pourovskii, J. Phys.: Condens. Matter **31**, 373001 (2019)

[160] K. Haule and G. Kotliar, New. J. Phys. **11**, 025021 (2009); A. Georges, L de'Medici, and J. Mravlje, Ann. Rev. Condens. Matter Phys. **4**, 137 (2013); D. Guterding, S. Backes, M. Tomić, H.O. Jeschke, and R. Valentí, Phys. Status Solidi B **254**, 1600164 (2017)

[161] R. Adler, C.-J. Kang, C.-H. Yee, and G. Kotliar, Rep. Prog. Phys. **82**, 012504 (2019)

[162] G.G. Pálsson and G. Kotliar, Phys. Rev. Lett. **80**, 4775 (1998); P. Wissgott, A. Toschi, H. Usui, K. Kuroki, and K. Held, Phys. Rev. B **82**, 201106(R) (2010); W. Xu, K. Haule, and G. Kotliar, Phys. Rev. Lett. **111**, 036401 (2013); M. Zingl, G.J. Kraberger, and M. Aichhorn, Phys. Rev. Mater. **3**, 075404 (2019)

[163] M.J. Han, X. Wang, C.A. Marianetti, A.J. Millis, Phys. Rev. Lett. **107**, 206804 (2011); J.K. Freericks, *Transport in multilayered nanostructures – The dynamical mean-field approach*, 2nd edition (Imperial College Press, London, 2016); Z. Zhong, M. Wallerberger, J.M. Tomczak, C. Taranto, N. Parragh, A. Toschi, G. Sangiovanni, K. Held, Phys. Rev. Lett. **114**, 246401 (2015); F. Lechermann, Phys. Rev. Mater. **2**, 085004 (2018)

[164] H. Chen, A. Hampel, J. Karp, F. Lechermann, A. Millis, Front. Phys. **10**, 835942 (2022)

[165] G. Rai, L. Crippa, D. Călugăru, H. Hu, F. Paoletti, L. de'Medici, A. Georges, B.A. Bernevig, R. Valentí, G. Sangiovanni, T. Wehling, Phys. Rev. X **14**, 031045 (2024)

[166] D. Jacob, K. Haule, and G. Kotliar, Phys. Rev. B **82**, 195115 (2010); L. Chioncel, C. Morari, A. Östlin, W.H. Appelt, A. Droghetti, M.M. Radonjić, I. Rungger, L. Vitos, U. Eckern, A.V. Postnikov, Phys. Rev. B **92**, 054431 (2015); M. Schüler, S. Barthel, T. Wehling, M. Karolak, A. Valli, and G. Sangiovanni, Eur. Phys. J. Spec. Top. **226**, 2615 (2017); P. Pudleiner, A. Kauch, K. Held, and G. Li, Phys. Rev. B **100**, 075108 (2019)

[167] C. Weber, D.D. O'Regan, N.D.M. Hine, P.B. Littlewood, G. Kotliar, and M.C. Payne, Phys. Rev. Lett. **110**, 106402 (2013); M.A. al-Badri, E. Linscott, A. Georges, D.J. Cole, and C. Weber, Commun. Phys. **3**, 4 (2020)